

Inverse spin-Hall effect and spin-swapping in spin-split superconductors

Lina Johnsen Kamra* and Jacob Linder

Center for Quantum Spintronics, Department of Physics, Norwegian
University of Science and Technology, NO-7491 Trondheim, Norway

(Dated: February 26, 2024)

When a spin-splitting field is introduced to a thin film superconductor, the spin currents polarized along the field couples to energy currents that can only decay via inelastic scattering. We study spin and energy injection into such a superconductor where spin-orbit impurity scattering yields inverse spin-Hall and spin-swapping currents. We show that the combined presence of a spin-splitting field, superconductivity, and inelastic scattering gives rise to a renormalization of the spin-Hall and spin-swap angles. In addition to an enhancement of the ordinary inverse spin-Hall effect, spin-splitting gives rise to unique inverse spin-Hall and spin-swapping signals five orders of magnitude stronger than the ordinary inverse spin-Hall signal. These can be completely controlled by the orientation of the spin-splitting field, resulting in a long-range charge and spin accumulations detectable much further from the injector than in the normal-state. Our results demonstrate that superconductors provide tunable inverse spin-Hall and spin-swapping signals with high detection sensitivity.

Introduction.—Superconductors, while fascinating on their own, exhibit emergent quantum phenomena in combination with magnetic materials that are pursued for technological applications and fundamental interest [1–6]. This includes phenomena such as extreme sensitivity to electromagnetic fields [7] and heat [8–11], infinite magnetoresistance effects [12, 13], qubits [14], and dissipationless flow of spin [15–17].

Enhancing spin-dependent transport via superconductors and enabling qualitatively new ways to utilize spins compared to non-superconducting systems is among the main aims of the field [18]. In superconductors, spin can be carried by the Cooper pair condensate *or* by quasi-particle excitations. The quasi-particles of a superconductor are qualitatively different from the non-superconducting state, in that their charge and velocity are highly energy-dependent while their spin is constant. This feature causes spin transport via quasi-particles to depend strongly on whether relaxation occurs via spin-orbit scattering or magnetic impurities [19–23]. A key component in spin transport is the manner in which spin currents are detected. This is customarily done by using the inverse spin-Hall effect [24, 25] where a spin current is converted into a transverse electric voltage. The efficiency of the spin-to-charge conversion is quantified by a spin-Hall angle θ_{SH} . For maximal detection sensitivity, it is desirable to make θ_{SH} as large as possible. Previous works have investigated the spin-Hall effect and its inverse in superconducting systems, predicting slightly enhanced inverse spin-Hall effects [26]. Experiments have observed an inverse spin-Hall effect that exceeded its normal-state value by three orders of magnitude [27, 28].

While magnetic fields can only penetrate a distance λ into a superconductor due to the Higgs mechanism [29–31], it is still possible to spin-polarize a superconducting thin film by making its thickness substantially smaller than λ [32]. This enables the study of an intriguing interplay between superconducting phase coherence and spin-polarization, which has been shown to cause large and tunable thermoelectric effects [11, 33, 34] as well as electron pairs with a coherence that is temporally non-local [35, 36]. The superconducting quasi-particles are affected by the spin-polarization, which renormalizes the impurity self-

energies in a superconductor [37–39] and could have a profound effect on the spin-Hall effect and its inverse. However, this has not been investigated so far. Finding a way to substantially increase the spin-Hall effect by using superconductors would be an important result due to widespread use of spin currents in spintronics and related fields.

Here, we use Keldysh non-equilibrium Green’s function theory [40–42] to compute the inverse spin-Hall response of a spin-split superconductor. Additionally, we compute the spin-swapping properties [43] of such a system – the conversion of a spin-polarized current flowing in one direction to a differently polarized spin-current flowing in a perpendicular direction. We find that the spin-splitting field not only renormalizes some transversal currents, but can lead to strong and tunable inverse spin-Hall and spin-swapping signals unique to the spin-split superconductor.

Theory.—We consider a superconductor connected to a normal-metal contact. When applying a spin-polarized voltage, both spin and energy quasi-particle currents are injected into the superconductor. The spin current decays inside the superconductor due to ordinary, spin-orbit, spin-flip, and inelastic scattering, while the energy current can only decay through inelastic scattering [4]. The spin-orbit scattering can also generate transversal currents through the inverse spin-Hall and spin-swap effects. We here study the transversal currents in the presence of a spin-splitting field.

To do so, we consider the Usadel equation $\nabla_{\mathbf{R}} \cdot \tilde{\mathbf{J}}(\mathbf{R}, \epsilon) = i[\tilde{\sigma}(\mathbf{R}, \epsilon), \tilde{g}_{\text{av}}^s(\mathbf{R}, \epsilon)] + \tilde{\mathcal{T}}(\mathbf{R}, \epsilon)$ for the Keldysh space Green’s function $\tilde{g}_{\text{av}}^s(\mathbf{R}, \epsilon)$ including a matrix current [38, 39, 44] with first order corrections in the spin-orbit parameter α

$$\tilde{\mathbf{J}}(\mathbf{R}, \epsilon) = -D \left(-\frac{i\kappa}{2} \{ \hat{\rho}_3 \hat{\sigma} \times \tilde{g}_{\text{av}}^s(\mathbf{R}, \epsilon) \nabla_{\mathbf{R}} \tilde{g}_{\text{av}}^s(\mathbf{R}, \epsilon) \} - \frac{\theta}{2} [\hat{\rho}_3 \hat{\sigma} \times \nabla_{\mathbf{R}} \tilde{g}_{\text{av}}^s(\mathbf{R}, \epsilon)] + \tilde{g}_{\text{av}}^s(\mathbf{R}, \epsilon) \nabla_{\mathbf{R}} \tilde{g}_{\text{av}}^s(\mathbf{R}, \epsilon) \right). \quad (1)$$

For its derivation and additional details about the calculation, physical observables, and the choice of parameters, see the Supplemental Material (SM). The normal-state spin-Hall and spin-swap angles θ and κ are proportional to α . Above,

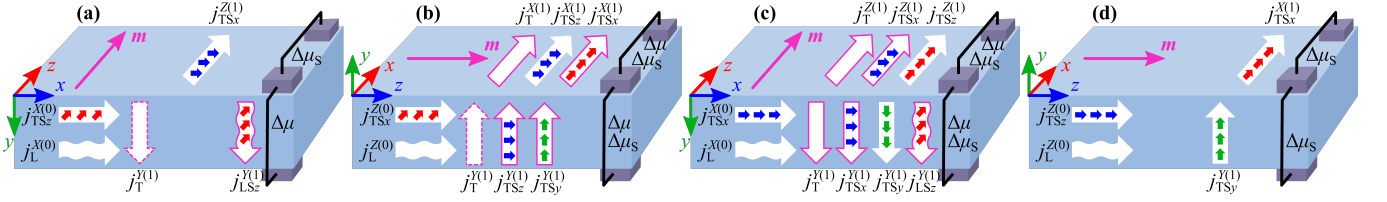


FIG. 1. We inject a spin current $\mathbf{j}_{\text{TS}x_i}^{(0)}$ polarized along x_i and an energy current $\mathbf{j}_L^{(0)}$ (big horizontal arrows) into a spin-split superconductor with an in-plane spin-splitting field \mathbf{m} (pink arrow). In panel (a) and (b), the spin polarization (small arrows) of the injected spin current is perpendicular to the current direction, and in panel (c) and (d), it is parallel. From panel (a) to (b), and from panel (c) to (d), the spin-splitting field is rotated by $\pi/2$. We also rotate the coordinate system so that $\mathbf{m} = m\mathbf{z}$. This way, the energy current is always coupled to the z polarized spin current. The injected currents produce transversal charge and spin currents through the inverse spin-Hall and spin-swap effects. The transversal currents that are present only in a spin-split superconductor are outlined by a pink solid line, and those that are renormalized by the spin-splitting field are outlined by a dashed pink line. The transversal charge and z polarized spin-energy currents $\mathbf{j}_T^{(1)}$ and $\mathbf{j}_{\text{LS}z}^{(1)}$ produce charge accumulations $\Delta\mu$. The transversal spin currents $\mathbf{j}_{\text{TS}x_i}^{(1)}$ produce spin accumulations $\Delta\mu_s$. Transversal energy currents could in principle contribute to the z polarized spin accumulation, but these cannot be generated from the injected spin and energy currents. Note that although the white arrows point in the positive current direction, the directions of the currents can be positive or negative depending on the parameters.

$D = \tau v_F^2/3$ is the diffusion coefficient determined by the scattering time τ and the Fermi velocity v_F . The torque $\tilde{\mathcal{T}}(\mathbf{R}, \epsilon)$ arises from the first order corrections in the spin-orbit scattering, but only gives a nonzero contribution in the presence of supercurrents. We assume the retarded part of the Green's function to be constant in space, focusing only on the quasi-particle transport. The self-energy $\tilde{\sigma}(\mathbf{R}, \epsilon)$ of a spin-split superconductor is given by $\hat{\sigma}_{\text{ssSC}}(\epsilon) = \epsilon\hat{\rho}_3 + \hat{\Delta} - \hat{\rho}_0\boldsymbol{\sigma} \cdot \mathbf{m}$, where ϵ is the energy, $\hat{\Delta} = \text{diag}(\Delta, -\Delta, \Delta^*, -\Delta^*)$ is the matrix introducing the superconducting gap Δ , and \mathbf{m} is the spin-splitting field. Additionally, we include spin-orbit, spin-flip, and inelastic scattering, respectively, through the self-energy terms $\hat{\sigma}_{\text{so}}(\mathbf{R}, \epsilon) = \frac{i}{8\tau_{\text{so}}}\hat{\rho}_3\hat{\boldsymbol{\sigma}} \cdot \hat{\mathbf{g}}_{\text{av}}^s(\mathbf{R}, \epsilon)\hat{\rho}_3\hat{\boldsymbol{\sigma}}$, $\hat{\sigma}_{\text{sf}}(\mathbf{R}, \epsilon) = \frac{i}{8\tau_{\text{sf}}}\hat{\boldsymbol{\sigma}} \cdot \hat{\mathbf{g}}_{\text{av}}^s(\mathbf{R}, \epsilon)\hat{\boldsymbol{\sigma}}$, and $\hat{\sigma}_{\text{isc}}(\epsilon) = i\delta\text{diag}(\hat{\rho}_3, -\hat{\rho}_3) + 2i\delta \tanh(\frac{\epsilon}{2T})\text{antidiag}(\hat{\rho}_3, 0)$. Here, τ_{so} and τ_{sf} are the spin-orbit and spin-flip scattering times, δ is a small parameter determining the strength of the inelastic scattering, and T is the temperature. We have defined the matrices $\hat{\rho}_3 = \text{diag}(1, 1, -1, -1)$, $\hat{\rho}_0 = \text{diag}(1, 1, 1, 1)$, and $\hat{\boldsymbol{\sigma}} = \text{diag}(\boldsymbol{\sigma}, \boldsymbol{\sigma}^*)$, where $\boldsymbol{\sigma}$ is the vector of Pauli matrices.

From the above, we derive the non-equilibrium charge and spin accumulation across the superconductor resulting from the transversal currents. We choose to fix the spin-splitting field along z . In this case, the energy current always couples to the z polarized spin current, and the charge current always couples to the z polarized spin-energy current. The x and y polarized spin currents are also coupled together due to the precession of the spin around the spin-splitting field [4]. In the following, we present expressions for the transversal currents $\mathbf{j}^{(1)}$ relevant for the charge and spin accumulations in terms of the injected currents $\mathbf{j}^{(0)}$. These are derived from the Keldysh part of the matrix current in Eq. (1), and are a result of the first and zeroth order terms in the spin-orbit parameter α , respectively.

The inverse spin-Hall effect.—In the inverse spin-Hall effect, a transversely polarized spin current is transformed into a transversal charge current resulting in a non-equilibrium charge accumulation across the superconductor [24, 25]. In spin-split superconductors, the charge accumulation can also have a contribution from a spin-energy current with spin polarization

parallel to the spin-splitting field [4]. We first study how the inverse spin-Hall effect is renormalized in a spin-split superconductor (ssSC) compared to a superconductor (SC) and a normal-metal (NM), and then consider charge accumulations that only occur in the presence of spin-splitting.

If the spin polarization of the injected current and the spin-splitting field are both oriented along z and perpendicular to the direction of the injected current x , the transversal charge current is out-of-plane (OOP) and given by

$$\mathbf{j}_T^{Y(1)}(x, \epsilon) = -\theta_{\text{SH}}^\perp(\epsilon)\mathbf{j}_{\text{TS}z}^{X(0)}(x, \epsilon) + \theta_{\text{EH}}^\perp(\epsilon)\mathbf{j}_L^{X(0)}(x, \epsilon), \quad (2)$$

with the spin-Hall angle

$$\theta_{\text{SH}}^\perp(\epsilon) = \begin{cases} \theta D \frac{N_+(\epsilon)D_L(\epsilon) - N_-(\epsilon)D_{\text{TS}z}(\epsilon)}{[D_L(\epsilon)]^2 - [D_{\text{TS}z}(\epsilon)]^2} & \text{for a ssSC,} \\ \theta DN(\epsilon)/D_L(\epsilon) & \text{for a SC,} \\ \theta & \text{for a NM,} \end{cases} \quad (3)$$

and the energy-Hall angle

$$\theta_{\text{EH}}^\perp(\epsilon) = \begin{cases} \theta D \frac{N_+(\epsilon)D_{\text{TS}z}(\epsilon) - N_-(\epsilon)D_L(\epsilon)}{[D_L(\epsilon)]^2 - [D_{\text{TS}z}(\epsilon)]^2} & \text{for a ssSC,} \\ 0 & \text{for a SC and a NM.} \end{cases} \quad (4)$$

The OOP spin-energy current that also contributes to the charge accumulation is given by

$$\mathbf{j}_{\text{LS}z}^{Y(1)}(x, \epsilon) = -\theta_{\text{SH}}^\perp(\epsilon)\mathbf{j}_L^{X(0)}(x, \epsilon) + \theta_{\text{EH}}^\perp(\epsilon)\mathbf{j}_{\text{TS}z}^{X(0)}(x, \epsilon). \quad (5)$$

These OOP currents are illustrated in Fig. 1(a). Above, $N_+(\epsilon)$ and $N(\epsilon)$ are the density-of-states (DOS) normalized by their normal-state value in the ssSC and SC, respectively, $D_L(\epsilon) = D$ in the normal-state, and $N_-(\epsilon)$ and $D_{\text{TS}z}(\epsilon)$ are only non-zero in the presence of spin-splitting. Complete expressions are given in the SM. The above spin-Hall and energy-Hall angles are plotted in Fig. 2(a). Inelastic scattering allows for a two orders of magnitude increase in the spin-Hall and energy-Hall angles below the gap edge of the SC. In the presence of a spin-splitting field where the gap edges of the spin-up and spin-down quasi-particles are shifted with respect to each other,

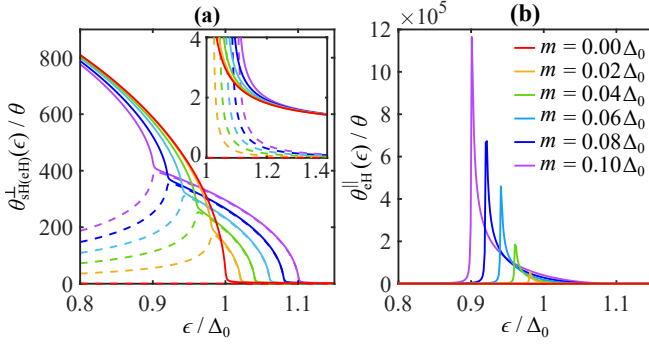


FIG. 2. (a) The spin-Hall angle $\theta_{\text{SH}}^{\perp}$ (solid lines) and the energy-Hall angle $\theta_{\text{eH}}^{\perp}$ (dashed lines) for various spin-splitting fields m . Due to inelastic scattering, there is a huge renormalization of $\theta_{\text{SH}}^{\perp}(\epsilon)$ and $\theta_{\text{eH}}^{\perp}(\epsilon)$ below the outer gap edge (rightmost kink). Above the outer gap, where both spin-up and spin-down quasi-particles are present, there is a weaker renormalization (inset). At large energies, $\theta_{\text{SH}}^{\perp}(\epsilon) \rightarrow \theta$ and $\theta_{\text{eH}}^{\perp}(\epsilon) \rightarrow 0$. (b) The energy-Hall angle $\theta_{\text{eH}}^{\parallel}$ is strongly renormalized between the inner and outer gap edge. At large energies, $\theta_{\text{eH}}^{\parallel}(\epsilon) \rightarrow 0$. Note that $\theta_{\text{SH}}^{\perp}(\epsilon)$ is even in energy, while $\theta_{\text{eH}}^{\perp}(\epsilon)$ and $\theta_{\text{eH}}^{\parallel}(\epsilon)$ are odd in energy. The energy is normalized by the zero-temperature superconducting gap Δ_0 at $m = 0$, while the angles are normalized by the normal-state spin-Hall angle θ . We consider zero temperature, so that $\Delta = \Delta_0$ at $m = 0$.

there is also a large renormalization for energies between the inner and outer gap edges in the DOS. There is also a smaller increase in the spin-Hall and energy-Hall angles above the outer gap where both spin-species are present.

If we rotate the magnetic field so that it is parallel to the propagation direction, there is no spin-energy current contribution to the charge accumulation and the charge current is instead given by

$$j_{\text{T}}^{Y(1)}(z, \epsilon) = \theta_{\text{SH}}^x(\epsilon) j_{\text{TSx}}^{Z(0)}(z, \epsilon) - \theta_{\text{SH}}^y(\epsilon) j_{\text{TSy}}^{Z(0)}(z, \epsilon). \quad (6)$$

We have now defined the propagation direction of the injected current along z and its spin along x . The precession of the spin around the spin-splitting field results in two spin-Hall angles for the current polarized along x and y ,

$$\theta_{\text{SH}}^x(\epsilon) = \begin{cases} \theta D \frac{N_+(\epsilon) D_{\text{TSx}}(\epsilon) + N_-^{\perp}(\epsilon) D_{\text{TSy}}(\epsilon)}{[D_{\text{TSx}}(\epsilon)]^2 + [D_{\text{TSy}}(\epsilon)]^2} & \text{for a ssSC,} \\ \theta_{\text{SH}}(\epsilon) & \text{for a SC and a NM,} \end{cases} \quad (7)$$

$$\theta_{\text{SH}}^y(\epsilon) = \begin{cases} \theta D \frac{N_+(\epsilon) D_{\text{TSy}}(\epsilon) - N_-^{\perp}(\epsilon) D_{\text{TSx}}(\epsilon)}{[D_{\text{TSx}}(\epsilon)]^2 + [D_{\text{TSy}}(\epsilon)]^2} & \text{for a ssSC,} \\ 0 & \text{for a SC and a NM.} \end{cases} \quad (8)$$

Above, $D_{\text{TSx}}(\epsilon) = D_{\text{TSz}}(\epsilon)$ in the absence of spin-splitting, while $N_-^{\perp}(\epsilon)$ and $D_{\text{TSy}}(\epsilon)$ are only non-zero in the presence of spin-splitting. The OOP charge current is illustrated in Fig. 1(b). When increasing the spin-splitting field, the above spin-Hall angles are suppressed compared to $\theta_{\text{SH}}^{\perp}(\epsilon)$. The renormalization of the OOP charge accumulation therefore changes when we rotate the spin-splitting field between the configurations in Fig. 1(a) and (b).

We next consider charge accumulations that only appear in the presence of spin-splitting. Consider the case where the spin

of the injected current is parallel to its propagation direction x , and the spin-splitting field is perpendicular to these. In this case, we find OOP charge and spin-energy currents

$$j_{\text{T}}^{Y(1)}(x, \epsilon) = -\theta_{\text{eH}}^{\parallel} j_{\text{L}}^{X(0)}(x, \epsilon), \quad (9)$$

$$j_{\text{LSz}}^{Y(1)}(x, \epsilon) = -[N_+(\epsilon)/N_-(\epsilon)] \theta_{\text{eH}}^{\parallel} j_{\text{L}}^{X(0)}(x, \epsilon) \quad (10)$$

that only have a contribution from the injected energy current. The energy-Hall angle is given by

$$\theta_{\text{eH}}^{\parallel} = \begin{cases} \theta D \frac{N_-(\epsilon) D_{\text{L}}(\epsilon)}{[D_{\text{L}}(\epsilon)]^2 - [D_{\text{TS}}(\epsilon)]^2}, & \text{for a ssSC,} \\ 0 & \text{for a SC and a NM.} \end{cases} \quad (11)$$

Note that while the spin-energy current is finite also in the absence of spin-splitting due to $N_+(\epsilon)$ being finite, it only gives a contribution to the charge accumulation in the presence of spin-splitting. The above OOP charge and spin-energy currents are illustrated in Fig. 1(c). They disappear when rotating the spin-splitting field to the parallel orientation, as shown in Fig. 1(d). The corresponding energy-Hall angle is plotted in Fig. 2(b). Due to the inelastic scattering, there is a huge renormalization between the inner and outer gap edges. The angle of the spin-energy current is renormalized in the same way between the inner and outer gap, but is instead odd in energy.

Additionally, in-plane (IP) charge currents

$$j_{\text{T}}^{X(1)}(z, \epsilon) = -\theta_{\text{SH}}^x(\epsilon) j_{\text{TSy}}^{Z(0)}(z, \epsilon) - \theta_{\text{SH}}^y(\epsilon) j_{\text{TSx}}^{Z(0)}(z, \epsilon), \quad (12)$$

$$j_{\text{T}}^{Z(1)}(x, \epsilon) = \theta_{\text{SH}}^x(\epsilon) j_{\text{TSy}}^{X(0)}(x, \epsilon) + \theta_{\text{SH}}^y(\epsilon) j_{\text{TSx}}^{X(0)}(x, \epsilon), \quad (13)$$

exist when the spin-splitting field is perpendicular to the injected spin, regardless of their orientation with respect to the direction of the injected current. This is shown in Fig. 1(b) and (c), respectively. These currents disappear when rotating the spin-splitting field by $\pi/2$, see Fig. 1(a) and (d). Thus, several transversal currents appear that are only present in a spin-split superconductor and can be controlled by the orientation of the spin-splitting field.

Spin-swapping.—A spin-swap current is a transversal spin current that appear due to an injected spin current [43]. As a result, there is a non-equilibrium spin-accumulation across the superconductor. While the normal-state spin-swap currents are neither renormalized by superconductivity nor spin-splitting, unique spin-swap currents appear in the superconductor that are only present under a spin-splitting field.

We first consider transversal currents where the propagation direction and spin polarization are perpendicular to each other. If we inject a spin current with spin polarization and propagation direction along the x_i and x_j axes, respectively, we produce an IP spin-swap current $j_{\text{TSx}_j}^{X_i(1)}(X_j, \epsilon) = -\kappa j_{\text{TSx}_i}^{X_j(0)}(X_j, \epsilon)$ where the indices i and j are swapped compared to the incoming current. This is illustrated in Fig. 1(a) and (b). When the spin-splitting field is perpendicular to the spin-polarization of the injected current, an additional OOP spin-swap current appears, as shown in Fig. 1(b) and (c). These still follow the

same expression as above, but are absent when rotating the spin-splitting field by $\pi/2$ to the configuration in Fig. 1(a) and (d), respectively. In the case when the spin polarization of the injected current is along the current direction, but the spin-splitting field is perpendicular to these, we find an IP spin current $j_{\text{TS}x}^{Z(1)}(x, \epsilon) = -\kappa_{\text{es}} j_L^{X(0)}(x, \epsilon)$ with spin-swap angle

$$\kappa_{\text{es}} = \begin{cases} \kappa \frac{D_L(\epsilon) D_{\text{TS}}^z(\epsilon)}{[D_L(\epsilon)]^2 - [D_{\text{TS}}^z(\epsilon)]^2} & \text{for a ssSC,} \\ 0 & \text{for a SC and a NM,} \end{cases} \quad (14)$$

where only the energy current contributes. This IP current is shown in Fig. 1(c), and disappears when the spin-splitting field is rotated to the configuration in Fig. 1(d). The above spin-swap angle is only non-zero below the outer gap edge, and is greatly renormalized between the inner and outer gap edges similar to the energy-Hall angle in Fig. 2(b).

We next consider the transversal currents that carry spin polarized along their propagation direction. As a result of an incoming spin current polarized along its propagation direction, we find IP and OOP transversal spin-currents $j_{\text{TS}x_i}^{X_i(1)}(X_j, \epsilon) = \kappa j_{\text{TS}x_j}^{X_j(0)}(X_j, \epsilon)$ that only depend on the injected spin-current via the normal-state spin-swap angle, see Fig. 1(c) and (d). However, similar currents also appear when the spin polarization of the injected current is perpendicular to its propagation direction if the spin-splitting field is parallel to the incoming current. In this case, only the energy current contributes to the transversal spin-currents $j_{\text{TS}x_i}^{X_i(1)}(z, \epsilon) = \kappa_{\text{es}} j_L^{Z(0)}(z, \epsilon)$ through a strongly renormalized spin-swap coefficient. These currents are illustrated in Fig. 1(b), and disappear in Fig. 1(a) where the spin-splitting field is rotated. Although the ordinary spin-swap angles are unaffected by spin-splitting and superconductivity, additional transversal currents appear that either depend on the normal-state spin-swap angle or a strongly renormalized one.

Charge and spin accumulations.—We next study the resulting non-equilibrium charge and spin accumulations measured across the transversal IP and OOP directions of the system. We focus on the cases where the spin-splitting couples the transversal currents to the injected energy current that can only decay by inelastic scattering. Since the inelastic scattering rate is typically much slower than the spin-orbit and spin-flip scattering rates, the energy current survives far into the superconductor compared to the injected spin current [4]. In Fig. 3(a) and (b), we show how the contribution from the long-range energy current gives rise to an inverse spin-Hall signal that survives far inside the spin-split superconductor. Without coupling between the injected spin and energy currents, the charge accumulation is small because spin injection is forbidden below the superconducting gap and decays rapidly because the quasi-particle spin currents are sensitive to spin-flip scattering [20, 23]. Similar to our predictions, large inverse spin-Hall signals have recently been observed experimentally in spin-split superconductors [28].

As shown in Fig. 3(c) and (d), charge and spin accumulations five orders of magnitude larger than the ordinary inverse

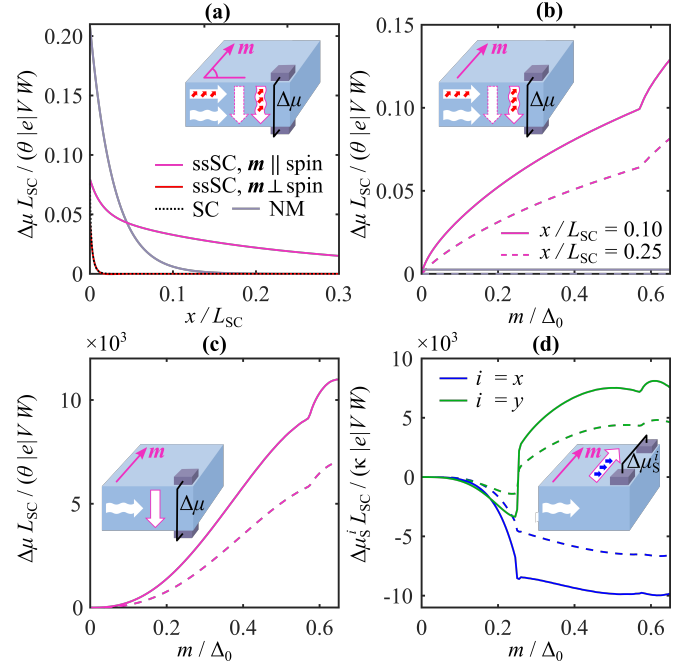


FIG. 3. (a) When the injected spin is oriented along the spin-splitting field ($\mathbf{m} \parallel \text{spin}$, Fig. 1(a)), the OOP charge accumulation $\Delta\mu$ can be detected for much longer distances inside a spin-split superconductor (ssSC) than inside a normal-metal (NM). When the spin-splitting field is rotated by $\pi/2$ ($\mathbf{m} \perp \text{spin}$, Fig. 1(b)), the charge accumulation is strongly suppressed and behaves as in the absence of spin-splitting (SC). The charge accumulation is normalized by $\theta|e|VW/L_{\text{SC}}$, where θ is the normal-state spin-Hall angle, e is the electron charge, $V = (V_{\uparrow} - V_{\downarrow})$ is the spin-voltage in the injector, W is the distance between the detectors, and L_{SC} is the length of the ssSC. We consider a spin-splitting field of magnitude $m = 0.1\Delta_0$, where Δ_0 is the zero-temperature gap at $m = 0$. (b) The charge accumulation increases with increasing spin-splitting field. (c) A charge accumulation five orders of magnitude larger than in panel (b) can be obtained in the configuration in Fig. 1(c) due to the huge renormalization of the spin-Hall angle shown in Fig. 2(b). (d) A spin accumulation $\Delta\mu_S^{x(y)}$ of the same order of magnitude results from the IP spin current $j_{\text{TS}x}^{Z(1)}$ in Fig. 1(c). Spin accumulations in Fig. 1(b) resulting from $j_{\text{TS}x}^{X(1)}(j_{\text{TS}y}^{Y(1)})$ are obtained by letting $\Delta\mu_S^x, \Delta\mu_S^y \rightarrow -\Delta\mu_S^x, -\Delta\mu_S^y$ ($-\Delta\mu_S^y, \Delta\mu_S^x$). For panel (b)-(d), solid and dotted curves refer to positions $x/L_{\text{SC}} = 0.10$ and $x/L_{\text{SC}} = 0.25$, respectively. We consider $|e|V = 2.5\Delta_0$, and $T = T_c/4$.

spin-Hall signal can be obtained as a result of the strongly renormalized spin-Hall and spin-swap angles in Eqs. (11) and (14). This is one of our main results. Due to inelastic scattering, these are massively renormalized between the inner and outer gap edges in the spin-split DOS, as demonstrated in Fig. 2(b). The enhancement happens when the spin-splitting field is oriented perpendicular to the spin of the injected spin current so that only the energy current contributes to the detected signal. Complete control of these inverse spin-Hall and spin-swap signals can thus be obtained by rotation of the spin-splitting field.

Concluding remarks.—In addition to a renormalization of the inverse spin-Hall signal, we find that a spin-splitting field

leads to inverse spin-Hall and spin-swap signals that do not appear in the absence of spin-splitting. Through charge and spin accumulations five orders of magnitude larger than the ordinary inverse spin-Hall signal, these unique signals offer major improvements in detection sensitivity. The dependence on the orientation of the spin-splitting field further allows for complete control of the measured signals.

Acknowledgments.—This work was supported by the Research Council of Norway through Grant No. 323766 and its Centres of Excellence funding scheme Grant No. 262633 “QuSpin.” Support from Sigma2 - the National Infrastructure for High Performance Computing and Data Storage in Norway, project NN9577K, is acknowledged.

* lina.g.johnsen@ntnu.no

- [1] F. S. Bergeret, A. F. Volkov, and K. B. Efetov, “Odd triplet superconductivity and related phenomena in superconductor-ferromagnet structures,” *Rev. Mod. Phys.* **77**, 1321–1373 (2005).
- [2] A. I. Buzdin, “Proximity effects in superconductor-ferromagnet heterostructures,” *Rev. Mod. Phys.* **77**, 935–976 (2005).
- [3] M. Eschrig, “Spin-polarized supercurrents for spintronics: A review of current progress,” *Rep. Prog. Phys.* **78**, 104501 (2015).
- [4] F. S. Bergeret, M. Silaev, P. Virtanen, and T. T. Heikkilä, “Colloquium: Nonequilibrium effects in superconductors with a spin-splitting field,” *Rev. Mod. Phys.* **90**, 041001 (2018).
- [5] D. S. Holmes and E. P. DeBenedictis, “Superconductor electronics and the international roadmap for devices and systems,” in *2017 16th International Superconductive Electronics Conference (ISEC)* (2017) pp. 1–3.
- [6] M. Amundsen, J. Linder, J. W. A. Robinson, I. Žutić, and N. Banerjee, “Colloquium: Spin-orbit effects in superconducting hybrid structures,” [arXiv:2210.03549](https://arxiv.org/abs/2210.03549) (2022).
- [7] R. C. Jaklevic, J. Lambe, A. H. Silver, and J. E. Mercereau, “Quantum interference effects in josephson tunneling,” *Phys. Rev. Lett.* **12**, 159–160 (1964).
- [8] M. S. Kalenkov, A. D. Zaikin, and L. S. Kuzmin, “Theory of a large thermoelectric effect in superconductors doped with magnetic impurities,” *Phys. Rev. Lett.* **109**, 147004 (2012).
- [9] P. Machon, M. Eschrig, and W. Belzig, “Nonlocal thermoelectric effects and nonlocal onsager relations in a three-terminal proximity-coupled superconductor-ferromagnet device,” *Phys. Rev. Lett.* **110**, 047002 (2013).
- [10] A. Ozaeta, P. Virtanen, F. S. Bergeret, and T. T. Heikkilä, “Predicted very large thermoelectric effect in ferromagnet-superconductor junctions in the presence of a spin-splitting magnetic field,” *Phys. Rev. Lett.* **112**, 057001 (2014).
- [11] S. Kolenda, M. J. Wolf, and D. Beckmann, “Observation of thermoelectric currents in high-field superconductor-ferromagnet tunnel junctions,” *Phys. Rev. Lett.* **116**, 097001 (2016).
- [12] D. Huertas-Hernando, Yu. V. Nazarov, and W. Belzig, “Absolute spin-valve effect with superconducting proximity structures,” *Phys. Rev. Lett.* **88**, 047003 (2002).
- [13] B. Li, N. Roschewsky, B. A. Assaf, M. Eich, M. Epstein-Martin, D. Heiman, M. Münzenberg, and J. S. Moodera, “Superconducting spin switch with infinite magnetoresistance induced by an internal exchange field,” *Phys. Rev. Lett.* **110**, 097001 (2013).
- [14] A. K. Feofanov, V. A. Oboznov, V. V. Bol’ginov, J. Lisenfeld, S. Poletto, V. V. Ryazanov, A. N. Rossolenko, M. Khabipov, D. Balashov, A. B. Zorin, P. N. Dmitriev, V. P. Koshelets, and A. V. Ustinov, “Implementation of superconductor/ferromagnet/superconductor π -shifters in superconducting digital and quantum circuits,” *Nat. Phys.* **6**, 593–597 (2010).
- [15] R. S. Keizer, S. T. B. Goennenwein, T. M. Klapwijk, G. Miao, and A. Gupta, “A spin triplet supercurrent through the half-metallic ferromagnet CrO_2 ,” *Nature* **439**, 825–827 (2006).
- [16] T. S. Khaire, M. A. Khasawneh, W. P. Pratt, and N. O. Birge, “Observation of spin-triplet superconductivity in Co-based Josephson junctions,” *Phys. Rev. Lett.* **104**, 137002 (2010).
- [17] J. W. A. Robinson, J. D. S. Witt, and M. G. Blamire, “Controlled injection of spin-triplet supercurrents into a strong ferromagnet,” *Science* **329**, 59–61 (2010).
- [18] J. Linder and J. W. A. Robinson, “Superconducting spintronics,” *Nat. Phys.* **11**, 307–315 (2015).
- [19] S. Takahashi and S. Maekawa, “Hall effect induced by a spin-polarized current in superconductors,” *Phys. Rev. Lett.* **88**, 116601 (2002).
- [20] J. P. Morten, A. Brataas, and W. Belzig, “Spin transport in diffusive superconductors,” *Phys. Rev. B* **70**, 212508 (2004).
- [21] M. Silaev, P. Virtanen, F. S. Bergeret, and T. T. Heikkilä, “Long-range spin accumulation from heat injection in mesoscopic superconductors with zeeman splitting,” *Phys. Rev. Lett.* **114**, 167002 (2015).
- [22] T. Wakamura, N. Hasegawa, K. Ohnishi, Y. Niimi, and Y. Otani, “Spin injection into a superconductor with strong spin-orbit coupling,” *Phys. Rev. Lett.* **112**, 036602 (2014).
- [23] L. G. Johnsen and J. Linder, “Spin injection and spin relaxation in odd-frequency superconductors,” *Phys. Rev. B* **104**, 144513 (2021).
- [24] M. I. D’yakonov and V. I. Perel, “Current-induced spin orientation of electrons in semiconductors,” *Phys. Lett. A* **35**, 459–460 (1971).
- [25] J. E. Hirsch, “Spin Hall effect,” *Phys. Rev. Lett.* **83**, 1834 (1999).
- [26] C. Espedal, P. Lange, S. Sadjina, A. G. Mal’shukov, and A. Brataas, “Spin Hall effect and spin swapping in diffusive superconductors,” *Phys. Rev. B* **95**, 054509 (2017).
- [27] T. Wakamura, H. Akaike, Y. Omori, Y. Niimi, S. Takahashi, A. Fujimaki, S. Maekawa, and Y. Otani, “Quasiparticle-mediated spin Hall effect in a superconductor,” *Nat. Mater.* **14**, 675 (2015).
- [28] K.-R. Jeon, J.-C. Jeon, X. Zhou, A. Migliorini, J. Yoon, and S. S. P. Parkin, “Giant transition-state enhancement of quasiparticle spin-hall effect in an exchange-spin-split superconductor detected by non-local magnon spin-transport,” *ACS Nano* **14**, 15784 (2020).
- [29] P. W. Anderson, “Plasmons, gauge invariance, and mass,” *Phys. Rev.* **130**, 439–442 (1963).
- [30] F. Englert and R. Brout, “Broken symmetry and the mass of gauge vector mesons,” *Phys. Rev. Lett.* **13**, 321–323 (1964).
- [31] P. W. Higgs, “Broken symmetries and the masses of gauge bosons,” *Phys. Rev. Lett.* **13**, 508–509 (1964).
- [32] R. Meservey and P. M. Tedrow, “Spin-polarized electron tunneling,” *Phys. Rep.* **238**, 173–243 (1994).
- [33] S. Kolenda, C. Sürgers, G. Fischer, and D. Beckmann, “Thermoelectric effects in superconductor-ferromagnet tunnel junctions on europium sulfide,” *Phys. Rev. B* **95**, 224505 (2017).
- [34] C. González-Ruano, D. Caso, J. A. Ouassou, C. Tiusan, Y. Lu, J. Linder, and F. G. Aliev, “Observation of magnetic state dependent thermoelectricity in superconducting spin valves,” [arXiv:2301.03263](https://arxiv.org/abs/2301.03263) (2023).
- [35] V. L. Berezinskii, “New model of the anisotropic phase of superfluid He_3 ,” *JETP Lett.* **20**, 628 (1974).
- [36] J. Linder and A. V. Balatsky, “Odd-frequency superconductivity,” *Rev. Mod. Phys.* **91**, 045005 (2019).
- [37] C. H. L. Quay, D. Chevallier, C. Bena, and M. Aprili, “Spin

- imbalance and spin-charge separation in a mesoscopic superconductor,” *Nat. Phys.* **9**, 84–88 (2013).
- [38] C. Huang, I. V. Tokatly, and F. S. Bergeret, “Extrinsic spin-charge coupling in diffusive superconducting systems,” *Phys. Rev. B* **98**, 144515 (2018).
 - [39] P. Virtanen, F. S. Bergeret, and I. V. Tokatly, “Magnetoelectric effects in superconductors due to spin-orbit scattering: Nonlinear σ -model description,” *Phys. Rev. B* **104**, 064515 (2021).
 - [40] J. W. Serene and D. Rainer, “The quasiclassical approach to superfluid ^3He ,” *Phys. Rep.* **101**, 221–311 (1983).
 - [41] J. Rammer and H. Smith, “Quantum field-theoretical methods in transport theory of metals,” *Rev. Mod. Phys.* **58**, 323–359 (1986).
 - [42] W. Belzig, F. K. Wilhelm, C. Bruder, G. d. Schön, and A. D. Zaikin, “Quasiclassical Green’s function approach to mesoscopic superconductivity,” *Superlatt. Microstruct.* **25**, 1251–1288 (1999).
 - [43] M. B. Lifshits and M. I. Dyakonov, “Swapping spin currents: Interchanging spin and flow directions,” *Phys. Rev. Lett.* **103**, 186601 (2009).
 - [44] F. S. Bergeret and I. V. Tokatly, “Manifestation of extrinsic spin Hall effect in superconducting structures: Nondissipative magnetoelectric effects,” *Phys. Rev. B* **94**, 180502 (2016).

SUPPLEMENTAL MATERIAL

We here outline the derivation of the Usadel equation with corrections to the first order in the spin-orbit parameter α (Sec. I), provide details about the numerical solution of the kinetic equations (Sec. II), and give expressions for the non-equilibrium charge and spin accumulations (Sec. III).

I. The Usadel equation

Our starting point for deriving the Usadel equation given in Eq. (1) in the main text is the continuum Hamiltonian

$$H(\mathbf{r}, t) = \int d\mathbf{r} \sum_{\sigma} \psi_{\sigma}^{\dagger}(\mathbf{r}, t) \left(-\frac{1}{2m} \nabla_{\mathbf{r}}^2 - \mu \right) \psi_{\sigma}(\mathbf{r}, t) + \frac{1}{2} \int d\mathbf{r} [\Delta(\mathbf{r}) \psi_{\uparrow}^{\dagger}(\mathbf{r}, t) \psi_{\downarrow}^{\dagger}(\mathbf{r}, t) + \text{h.c.}] \\ + \int d\mathbf{r} \sum_{\sigma, \sigma'} \psi_{\sigma}^{\dagger}(\mathbf{r}, t) [\mathbf{m}(\mathbf{r}) \cdot \boldsymbol{\sigma}]_{\sigma, \sigma'} \psi_{\sigma'}(\mathbf{r}, t) + \int d\mathbf{r} \sum_{\sigma, \sigma'} \psi_{\sigma}^{\dagger}(\mathbf{r}, t) U_{\sigma, \sigma'}^{\text{tot}}(\mathbf{r}) \psi_{\sigma'}(\mathbf{r}, t), \quad (15)$$

where $\psi_{\sigma}^{(\dagger)}(\mathbf{r}, t)$ is a field operator annihilating (creating) a spin- σ electron at position \mathbf{r} and time t . The first term includes the kinetic energy for electrons of mass m , and the chemical potential μ . The second term introduces superconductivity, where $\Delta(\mathbf{r}) = V \langle \psi_{\uparrow}(\mathbf{r}) \psi_{\downarrow}(\mathbf{r}) \rangle$ is the mean-field superconducting gap. The third term introduces a spin-splitting field $\mathbf{m}(\mathbf{r})$. The last term introduces the total scattering potential from the impurities $U_{\sigma, \sigma'}^{\text{tot}}(\mathbf{r})$. Above, $\boldsymbol{\sigma}$ is the vector of Pauli matrices.

We define the retarded, advanced and Keldysh Green's functions in Nambu \otimes spin space as

$$[\hat{G}^R(1, 2)]_{i,j} = -i\Theta(t_1 - t_2) \sum_k (\hat{\rho}_3)_{ik} \langle \{ [\psi(1)]_k, [\hat{\psi}^{\dagger}(2)]_j \} \rangle, \quad (16)$$

$$[\hat{G}^A(1, 2)]_{i,j} = i\Theta(t_2 - t_1) \sum_k (\hat{\rho}_3)_{ik} \langle \{ [\hat{\psi}(1)]_k, [\psi^{\dagger}(2)]_j \} \rangle, \quad (17)$$

$$[\hat{G}^K(1, 2)]_{i,j} = -i \sum_k (\hat{\rho}_3)_{ik} \langle [[\hat{\psi}(1)]_k, [\psi^{\dagger}(2)]_j] \rangle, \quad (18)$$

respectively, where $(1, 2)$ is short-hand notation for $(\mathbf{r}_1, t_1, \mathbf{r}_2, t_2)$, $\hat{\rho}_3 = \text{diag}(1, 1, -1, -1)$, and we have defined a basis

$$\hat{\psi}(\mathbf{r}, t) = [\psi_{\uparrow}(\mathbf{r}, t) \quad \psi_{\downarrow}(\mathbf{r}, t) \quad \psi_{\uparrow}^{\dagger}(\mathbf{r}, t) \quad \psi_{\downarrow}^{\dagger}(\mathbf{r}, t)]^T. \quad (19)$$

The above Green's functions are elements of the Keldysh space Green's function

$$\check{G}(1, 2) = \begin{pmatrix} \hat{G}^R(1, 2) & \hat{G}^K(1, 2) \\ 0 & \hat{G}^A(1, 2) \end{pmatrix}. \quad (20)$$

Before we start introducing higher order corrections, our approach follows the one described in Ref. [23]. From the Heisenberg equations of motion for the field operators, we find the equations of motion for the Keldysh space Green's function

$$[i\partial_{t_1} \hat{\rho}_3 - \hat{H}(\mathbf{r}_1)] \check{G}(1, 2) = \delta(1 - 2) \check{\rho}_0, \quad (21)$$

$$\check{G}(1, 2) [i\partial_{t_2} \hat{\rho}_3 - \hat{H}(\mathbf{r}_2) \hat{\rho}_3]^{\dagger} = \delta(1 - 2) \check{\rho}_0. \quad (22)$$

where

$$\hat{H}(\mathbf{r}) = \left(-\frac{1}{2m} \nabla_{\mathbf{r}}^2 - \mu \right) \hat{\rho}_0 - \hat{\Delta}(\mathbf{r}) + \hat{\tau}_0 \boldsymbol{\sigma} \cdot \mathbf{m}(\mathbf{r}) + \hat{U}_{\text{tot}}(\mathbf{r}). \quad (23)$$

Above, $\hat{\rho}_0$ is the 4×4 unit matrix, and $\hat{\tau}_0 \boldsymbol{\sigma} = \text{diag}(\boldsymbol{\sigma}, \boldsymbol{\sigma})$. The scattering potential matrix $\hat{U}_{\text{tot}}(\mathbf{r}) = U(\mathbf{r}) + \hat{U}_{\text{so}}(\mathbf{r}) + \hat{U}_{\text{sf}}(\mathbf{r})$ describe ordinary scattering on non-magnetic impurities, spin-orbit scattering on non-magnetic impurities, and spin-flip scattering on magnetic impurities, respectively. The scattering potentials are given by

$$U(\mathbf{r}) = \sum_i u(\mathbf{r} - \mathbf{r}_i), \quad (24)$$

$$\hat{U}_{\text{so}}(\mathbf{r}) = \sum_i i\alpha [\hat{\rho}_3 \hat{\boldsymbol{\sigma}} \times \nabla_{\mathbf{r}} u(\mathbf{r} - \mathbf{r}_i)] \cdot \nabla_{\mathbf{r}}, \quad (25)$$

$$\hat{U}_{\text{sf}}(\mathbf{r}) = \sum_i u_m(\mathbf{r} - \mathbf{r}_i) \hat{\boldsymbol{\sigma}} \cdot \mathbf{S}_i, \quad (26)$$

where $u(\mathbf{r} - \mathbf{r}_i)$ and $u_m(\mathbf{r} - \mathbf{r}_i)$ are the scattering potentials of a single non-magnetic and magnetic impurity at position \mathbf{r}_i , respectively, \mathbf{S}_i is the spin of the magnetic impurity, and $\hat{\sigma} = \text{diag}(\boldsymbol{\sigma}, \boldsymbol{\sigma}^*)$.

In order to solve Eqs. (21) and (22), we must replace the impurity potentials by self-energies. To do this, we split the Hamiltonian into two parts, $\hat{H}(\mathbf{r}) = \hat{H}_0(\mathbf{r}) + \hat{U}_{\text{tot}}(\mathbf{r})$, where $\hat{H}_0(\mathbf{r})$ describes the system in the absence of impurity scattering. The self-energies are introduced through the Dyson equations

$$\check{G}(1, 2) = \check{G}_0(1, 2) + \check{G}_0 \bullet \hat{\Sigma} \bullet \check{G}(1, 2), \quad (27)$$

$$\check{G}(1, 2) = \check{G}_0(1, 2) + \check{G} \bullet \hat{\Sigma}^\dagger \bullet \check{G}_0(1, 2), \quad (28)$$

where the self-energies are defined as $\hat{\Sigma}(1, 2) = \delta(1 - 2)\hat{U}_{\text{tot}}(\mathbf{r}_2)$. Above, $\check{G}_0(1, 2)$ is the Green's function in the absence of impurity scattering, and we have introduced the bullet product

$$A \bullet B(1, 2) = \int d3 A(1, 3)B(3, 2). \quad (29)$$

We solve the Dyson equations iteratively beyond the self-consistent Born approximation up to order $\mathcal{O}[(\hat{\Sigma} \bullet \check{G})^3]$ and $\mathcal{O}[(\check{G} \bullet \hat{\Sigma}^\dagger)^3]$ following a similar approach as Ref. [26, 38, 44]. Since we are not interested in one specific impurity configuration, we take the average over all impurities,

$$\langle \dots \rangle_{\text{av}} = \prod_{n=1}^N \left(\frac{1}{\mathcal{V}} \int d\mathbf{r}_n \right) \dots, \quad (30)$$

where \mathcal{V} is the volume of the system. We assume that the Green's function is approximately equal to its impurity-averaged value. By acting with $[i\partial_{t_1}\hat{\rho}_3 - \hat{H}_0(\mathbf{r}_1)]$ and $[i\partial_{t_2}\hat{\rho}_3 - \hat{\rho}_3\hat{H}_0(\mathbf{r}_2)\hat{\rho}_3]$ on the resulting equations, we obtain expressions similar to Eqs. (21) and (22), where the impurity potentials are replaced by expressions involving self-energies and impurity averaged Green's functions $\check{G}_{\text{av}}(1, 2)$. Subtracting the two equations, we find that

$$\begin{aligned} & [i\partial_{t_1}\hat{\rho}_3 - \hat{H}_0(\mathbf{r}_1)]\check{G}_{\text{av}}(1, 2) - \check{G}_{\text{av}}(1, 2)[i\partial_{t_2}\hat{\rho}_3 - \hat{\rho}_3\hat{H}_0(\mathbf{r}_2)\hat{\rho}_3]^\dagger \\ & - [\langle \hat{\Sigma} \bullet \check{G}_{\text{av}} \bullet \hat{\Sigma} \rangle_{\text{av}} \bullet \check{G}_{\text{av}}](1, 2) - [\langle \hat{\Sigma} \bullet \check{G}_{\text{av}} \bullet \hat{\Sigma} \bullet \check{G}_{\text{av}} \bullet \hat{\Sigma} \rangle_{\text{av}} \bullet \check{G}_{\text{av}}](1, 2) = 0. \end{aligned} \quad (31)$$

We will now make a series of approximations to this equation.

We first introduce center-of-mass and relative coordinates $\mathbf{R} = (\mathbf{r}_1 + \mathbf{r}_2)/2$ and $\mathbf{r} = \mathbf{r}_1 - \mathbf{r}_2$, and absolute and relative time coordinates $T = (t_1 + t_2)/2$ and $t = t_1 - t_2$. The Green's function is assumed to be independent of the absolute time coordinate. We introduce the Fourier transform and its inverse,

$$\check{G}_{\text{av}}(\mathbf{R}, \mathbf{p}, \epsilon) = \int d\mathbf{r} \int dt e^{-i\mathbf{p}\cdot\mathbf{r} + i\epsilon t} \check{G}_{\text{av}}(\mathbf{R}, \mathbf{r}, t), \quad (32)$$

$$\check{G}_{\text{av}}(\mathbf{R}, \mathbf{r}, t) = \int \frac{d\mathbf{p}}{(2\pi)^3} \int \frac{d\epsilon}{2\pi} e^{i\mathbf{p}\cdot\mathbf{r} - i\epsilon t} \check{G}_{\text{av}}(\mathbf{R}, \mathbf{p}, \epsilon). \quad (33)$$

Assuming all quantities to vary slowly compared to the Fermi wavelength, the Fourier transform of the bullet product between two functions $A(\mathbf{R}, \mathbf{p}, \epsilon)$ and $B(\mathbf{R}, \mathbf{p}, \epsilon)$ can be expressed through the first order gradient approximation

$$A \bullet B(\mathbf{R}, \mathbf{p}, \epsilon) = A(\mathbf{R}, \mathbf{p}, \epsilon)B(\mathbf{R}, \mathbf{p}, \epsilon) + \frac{i}{2} [\nabla_{\mathbf{R}} A(\mathbf{R}, \mathbf{p}, \epsilon) \cdot \nabla_{\mathbf{p}} B(\mathbf{R}, \mathbf{p}, \epsilon) - \nabla_{\mathbf{p}} A(\mathbf{R}, \mathbf{p}, \epsilon) \cdot \nabla_{\mathbf{R}} B(\mathbf{R}, \mathbf{p}, \epsilon)]. \quad (34)$$

Next, we assume that the absolute value of the momentum \mathbf{p} is approximately equal to the Fermi momentum p_F , so that we can apply the quasi-classical approximation

$$\int \frac{d\mathbf{p}}{(2\pi)^3} \check{G}_{\text{av}}(\mathbf{R}, \mathbf{p}, \epsilon) \approx N_0 \int d\xi_{p_F} \int \frac{d\mathbf{e}_{p_F}}{4\pi} \check{G}_{\text{av}}(\mathbf{R}, \mathbf{p}_F, \epsilon). \quad (35)$$

Above, N_0 is the DOS at the Fermi level, $\xi_{p_F} = p_F^2/2m$, and $\mathbf{e}_{p_F} = \mathbf{p}_F/p_F$ describes the direction of the momentum. We use the short-hand notation $\langle \dots \rangle_{p_F} = \int (d\mathbf{e}_{p_F}/4\pi)$ for the average over all directions of the momentum. We moreover introduce the quasi-classical Green's function

$$\check{g}_{\text{av}}(\mathbf{R}, \mathbf{p}_F, \epsilon) = \frac{i}{\pi} \int d\xi_{p_F} \check{G}_{\text{av}}(\mathbf{R}, \mathbf{p}_F, \epsilon). \quad (36)$$

In the diffusive limit, the quasi-classical Green's function can be approximated as

$$\check{g}_{\text{av}}(\mathbf{R}, \mathbf{p}_F, \epsilon) \approx \check{g}_{\text{av}}^s(\mathbf{R}, \epsilon) + \mathbf{e}_{p_F} \cdot \check{\mathbf{g}}_{\text{av}}^p(\mathbf{R}, \epsilon). \quad (37)$$

After applying all these approximations to Eq. (31), we separate out the even contributions in \mathbf{e}_{p_F} by averaging over all \mathbf{e}_{p_F} . We find that

$$\begin{aligned} & [\epsilon \hat{\rho}_3 + \hat{\Delta}(\mathbf{R}) - \hat{\rho}_0 \boldsymbol{\sigma} \cdot \mathbf{m}, \check{g}_{\text{av}}^s(\mathbf{R}, \epsilon)] + \frac{iv_F}{3} \nabla_{\mathbf{R}} \cdot \check{\mathbf{g}}_{\text{av}}^p(\mathbf{R}, \epsilon) \\ & - \int \frac{d\mathbf{e}_{p_F}}{4\pi} [\check{\sigma}_{\text{av}}^{\text{tot}}(\mathbf{R}, \mathbf{p}_F, \epsilon), \check{g}_{\text{av}}(\mathbf{R}, \mathbf{p}_F, \epsilon)] + \frac{i}{2} \int \frac{d\mathbf{e}_{p_F}}{4\pi} \nabla_{\mathbf{R}} \cdot \{ \nabla_{\mathbf{p}} \check{\sigma}_{\text{av}}^{\text{tot}}(\mathbf{R}, \mathbf{p}, \epsilon) \big|_{\mathbf{p}=\mathbf{p}_F}, \check{g}_{\text{av}}(\mathbf{R}, \mathbf{p}_F, \epsilon) \} = 0, \end{aligned} \quad (38)$$

where $v_F = p_F/m$ is the Fermi velocity. We next separate out the odd contributions in \mathbf{e}_{p_F} by multiplying the equation by \mathbf{e}_{p_F} before the averaging, which gives

$$\frac{1}{3} [\epsilon \hat{\rho}_3 + \hat{\Delta}(\mathbf{R}) - \hat{\rho}_0 \boldsymbol{\sigma} \cdot \mathbf{m}, \check{g}_{\text{av}}^p(\mathbf{R}, \epsilon)] + \frac{iv_F}{3} \nabla_{\mathbf{R}} \cdot \nabla_{\mathbf{R}} \check{g}_{\text{av}}^s(\mathbf{R}, \epsilon) - \int \frac{d\mathbf{e}_{p_F}}{4\pi} \mathbf{e}_{p_F} [\check{\sigma}_{\text{av}}^{\text{tot}}(\mathbf{R}, \mathbf{p}_F, \epsilon), \check{g}_{\text{av}}(\mathbf{R}, \mathbf{p}_F, \epsilon)] = 0. \quad (39)$$

We have included terms to the zeroth order in the gradient approximation in the odd equation and to first order in the even equation. The reason will become clear later on.

The most tricky part of solving Eqs. (38) and (39) is to evaluate the self-energies

$$\check{\sigma}_{\text{av}}^{\text{tot}}(\mathbf{R}, \mathbf{p}, \epsilon) = \langle \check{\Sigma} \bullet \check{G}_{\text{av}} \bullet \check{\Sigma} \rangle_{\text{av}}(\mathbf{R}, \mathbf{p}, \epsilon) + \langle \check{\Sigma} \bullet \check{G}_{\text{av}} \bullet \check{\Sigma} \bullet \check{G}_{\text{av}} \bullet \check{\Sigma} \rangle_{\text{av}}(\mathbf{R}, \mathbf{p}, \epsilon). \quad (40)$$

Our starting point is the real space expression for the self-energies

$$\begin{aligned} \check{\sigma}_{\text{av}}^{\text{tot}}(1, 2) &= \left(\prod_i \frac{1}{\nu} \int d\mathbf{r}_i \right) \hat{U}^{\text{tot}}(\mathbf{r}_1) \check{G}_{\text{av}}(1, 2) \hat{U}^{\text{tot}}(\mathbf{r}_2) \\ &+ \left(\prod_i \frac{1}{\nu} \int d\mathbf{r}_i \right) \int d3 \hat{U}^{\text{tot}}(\mathbf{r}_1) \check{G}_{\text{av}}(1, 3) \hat{U}^{\text{tot}}(\mathbf{r}_3) \check{G}_{\text{av}}(3, 2) \hat{U}^{\text{tot}}(\mathbf{r}_2) \end{aligned} \quad (41)$$

We neglect scatterings including more than one impurity (*i.e.* all of the impurity potentials in a single term has the same impurity index i). By following the same steps as described above for arriving at the even and odd equations, we find the following expressions for the self-energies:

1) For ordinary scattering to the second order in the impurity potential, the self-energy is

$$\check{\sigma}^{u^2}(\mathbf{R}, \mathbf{p}, \epsilon) = -\frac{i}{2} \left\langle \frac{1}{\tau(\mathbf{p} - \mathbf{q}_F)} \right\rangle_{q_F} \check{\mathbf{g}}_{\text{av}}^p(\mathbf{R}, \epsilon), \quad (42)$$

where we have defined

$$\left\langle \frac{1}{\tau(\mathbf{p} - \mathbf{q}_F)} \right\rangle_{q_F} = 2\pi n N_0 \langle |u(\mathbf{p} - \mathbf{q}_F)|^2 \rangle_{q_F}. \quad (43)$$

Above, n is the density of non-magnetic impurities.

2) When we combine one ordinary scattering and one spin-orbit scattering on the same non-magnetic impurity, the self-energy is

$$\begin{aligned} \check{\sigma}^{u u_{\text{so}}}(\mathbf{R}, \mathbf{p}, \epsilon) &= -\frac{i\alpha q_F}{12} \left\langle \frac{1}{\tau(\mathbf{p} - \mathbf{q}_F)} \right\rangle_{q_F} \nabla_{\mathbf{R}} \cdot [\hat{\rho}_3 \hat{\boldsymbol{\sigma}} \times \check{\mathbf{g}}_{\text{av}}^p(\mathbf{R}, \epsilon)] \\ &+ \frac{i\alpha}{4} \left\langle \frac{1}{\tau(\mathbf{p} - \mathbf{q}_F)} \right\rangle_{q_F} \{ \hat{\rho}_3 \hat{\boldsymbol{\sigma}} \times \mathbf{p} ; \nabla_{\mathbf{R}} \check{g}_{\text{av}}^s(\mathbf{R}, \epsilon) \} \\ &- \frac{\alpha q_F}{6} \left\langle \frac{1}{\tau(\mathbf{p} - \mathbf{q}_F)} \right\rangle_{q_F} \{ \hat{\rho}_3 \hat{\boldsymbol{\sigma}} \times \mathbf{p} ; \check{\mathbf{g}}_{\text{av}}^p(\mathbf{R}, \epsilon) \}. \end{aligned} \quad (44)$$

3) For two spin-orbit scatterings to the second order in the impurity potential, we get

$$\check{\sigma}^{u_{\text{so}}^2}(\mathbf{R}, \mathbf{p}, \epsilon) = -\frac{i\alpha^2 q_F^2}{6} \left\langle \frac{1}{\tau(\mathbf{p} - \mathbf{q}_F)} \right\rangle_{q_F} [p^2 \hat{\rho}_3 \hat{\boldsymbol{\sigma}} \cdot \check{g}_{\text{av}}^s(\mathbf{R}, \epsilon) \hat{\rho}_3 \hat{\boldsymbol{\sigma}} - (\mathbf{p} \cdot \hat{\rho}_3 \hat{\boldsymbol{\sigma}}) \check{g}_{\text{av}}^s(\mathbf{R}, \epsilon) (\mathbf{p} \cdot \hat{\rho}_3 \hat{\boldsymbol{\sigma}})]. \quad (45)$$

4) For ordinary scattering to the third order in the scattering potential, we get

$$\check{\sigma}^{u^3}(\mathbf{R}, \mathbf{p}, \epsilon) = \frac{1}{2\tau_{\text{sk}}(\mathbf{p})} \check{\rho}_0, \quad (46)$$

where we have defined

$$\frac{1}{\tau_{\text{sk}}(\mathbf{p})} = 2n(\pi N_0)^2 \langle u(\mathbf{p} - \mathbf{q}_F) u(\mathbf{q}_F - \mathbf{q}'_F) u(\mathbf{q}'_F - \mathbf{p}) \rangle_{q_F, q'_F}. \quad (47)$$

5) For two ordinary impurity scatterings and one spin-orbit impurity scattering on the same non-magnetic impurity, we get

$$\begin{aligned} \check{\sigma}^{u^2 u_{\text{so}}}(\mathbf{R}, \mathbf{p}, \epsilon) = & -\frac{\alpha}{4\tau_{\text{sk}}(\mathbf{p})} \mathbf{p} \cdot \{ \hat{\rho}_3 \hat{\boldsymbol{\sigma}} \times \check{g}_{\text{av}}^s(\mathbf{R}, \epsilon) \nabla_{\mathbf{R}} \check{g}_{\text{av}}^s(\mathbf{R}, \epsilon) \} \\ & - \frac{i\alpha p_F}{6\tau_{\text{sk}}(\mathbf{p})} \mathbf{p} \cdot [\hat{\rho}_3 \hat{\boldsymbol{\sigma}} \times \check{g}_{\text{av}}^s(\mathbf{R}, \epsilon) \check{g}_{\text{av}}^p(\mathbf{R}, \epsilon)] \\ & - \frac{\alpha p_F}{12\tau_{\text{sk}}(\mathbf{p})} \left\{ \hat{\rho}_3 \hat{\boldsymbol{\sigma}} \cdot [\nabla_{\mathbf{R}} \times \check{g}_{\text{av}}^p(\mathbf{R}, \epsilon)] \check{g}_{\text{av}}^s(\mathbf{R}, \epsilon) + \frac{1}{2} \check{g}_{\text{av}}^s(\mathbf{R}, \epsilon) \hat{\rho}_3 \hat{\boldsymbol{\sigma}} \cdot [\nabla_{\mathbf{R}} \times \check{g}_{\text{av}}^p(\mathbf{R}, \epsilon)] \right. \\ & \quad \left. + \frac{1}{2} [\nabla_{\mathbf{R}} \times \check{g}_{\text{av}}^p(\mathbf{R}, \epsilon)] \cdot \hat{\rho}_3 \hat{\boldsymbol{\sigma}} \check{g}_{\text{av}}^s(\mathbf{R}, \epsilon) + \check{g}_{\text{av}}^s(\mathbf{R}, \epsilon) [\nabla_{\mathbf{R}} \times \check{g}_{\text{av}}^p(\mathbf{R}, \epsilon)] \cdot \hat{\rho}_3 \hat{\boldsymbol{\sigma}} \right\} \\ & + \frac{\alpha p_F}{24\tau_{\text{sk}}(\mathbf{p})} \{ \check{g}_{\text{av}}^p(\mathbf{R}, \epsilon) \cdot [\hat{\rho}_3 \hat{\boldsymbol{\sigma}} \times \nabla_{\mathbf{R}} \check{g}_{\text{av}}^s(\mathbf{R}, \epsilon)] - [\nabla_{\mathbf{R}} \check{g}_{\text{av}}^s(\mathbf{R}, \epsilon) \times \hat{\rho}_3 \hat{\boldsymbol{\sigma}}] \cdot \check{g}_{\text{av}}^p(\mathbf{R}, \epsilon) \} \\ & + \frac{i\alpha p_F^2}{18\tau_{\text{sk}}(\mathbf{p})} \check{g}_{\text{av}}^p(\mathbf{R}, \epsilon) \cdot [\hat{\rho}_3 \hat{\boldsymbol{\sigma}} \times \check{g}_{\text{av}}^p(\mathbf{R}, \epsilon)] \\ & - \frac{i\alpha}{8\tau_{\text{sk}}(\mathbf{p})} \left([\nabla_{\mathbf{R}} \check{g}_{\text{av}}^s(\mathbf{R}, \epsilon)] \cdot \nabla_{\mathbf{p}} \{ \mathbf{p} \cdot [\nabla_{\mathbf{R}} \check{g}_{\text{av}}^s(\mathbf{R}, \epsilon) \times \hat{\rho}_3 \hat{\boldsymbol{\sigma}}] \} \right. \\ & \quad \left. + \nabla_{\mathbf{p}} \{ \mathbf{p} \cdot [\hat{\rho}_3 \hat{\boldsymbol{\sigma}} \times \nabla_{\mathbf{R}} \check{g}_{\text{av}}^s(\mathbf{R}, \epsilon)] \} \cdot [\nabla_{\mathbf{R}} \check{g}_{\text{av}}^s(\mathbf{R}, \epsilon)] \right) \\ & - \frac{\alpha p_F}{12\tau_{\text{sk}}(\mathbf{p})} \left([\nabla_{\mathbf{R}} \check{g}_{\text{av}}^s(\mathbf{R}, \epsilon)] \cdot \nabla_{\mathbf{p}} \{ \mathbf{p} \cdot [\check{g}_{\text{av}}^p(\mathbf{R}, \epsilon) \times \hat{\rho}_3 \hat{\boldsymbol{\sigma}}] \} \right. \\ & \quad \left. - \nabla_{\mathbf{p}} \{ \mathbf{p} \cdot [\hat{\rho}_3 \hat{\boldsymbol{\sigma}} \times \check{g}_{\text{av}}^p(\mathbf{R}, \epsilon)] \} \cdot [\nabla_{\mathbf{R}} \check{g}_{\text{av}}^s(\mathbf{R}, \epsilon)] \right). \end{aligned} \quad (48)$$

6) For two spin-flip scatterings on the same magnetic impurity, we get

$$\check{\sigma}^{u_{\text{sf}}^2}(\mathbf{R}, \mathbf{p}, \epsilon) = -\frac{iS(S+1)}{6} \left\langle \frac{1}{\tau_{\text{m}}(\mathbf{p} - \mathbf{q}_F)} \right\rangle_{q_F} \hat{\boldsymbol{\sigma}} \cdot \check{g}_{\text{av}}^s(\mathbf{R}, \epsilon) \hat{\boldsymbol{\sigma}}, \quad (49)$$

where S is the spin of the magnetic impurities, and

$$\left\langle \frac{1}{\tau_{\text{m}}(\mathbf{p} - \mathbf{q}_F)} \right\rangle_{q_F} = 2\pi n_{\text{m}} N_0 \langle |u_{\text{m}}(\mathbf{p} - \mathbf{q}_F)|^2 \rangle_{q_F}. \quad (50)$$

Above, n_{m} is the density of magnetic impurities. To obtain the expression for the spin-flip scattering self-energy, we have averaged over all directions of the magnetic moments.

Now that we have found expressions for all of the self-energies, we can proceed to evaluate the odd and even equations. The odd equation gives rise to the expression for the current matrix of the system. A common assumption is that the scattering on non-magnetic impurities dominates over all other terms. Using the normalization condition

$$\check{g}_{\text{av}}(\mathbf{R}, p_F, \epsilon) \check{g}_{\text{av}}(\mathbf{R}, p_F, \epsilon) = \check{\rho}_0 \quad (51)$$

when evaluating the odd equation, we can express $\check{g}_{\text{av}}^p(\mathbf{R}, \epsilon)$ in terms of $\check{g}_{\text{av}}^s(\mathbf{R}, \epsilon)$ as $\check{g}_{\text{av}}^p(\mathbf{R}, \epsilon) = -\tau v_F \check{g}_{\text{av}}^s(\mathbf{R}, \epsilon) \nabla_{\mathbf{R}} \check{g}_{\text{av}}^s(\mathbf{R}, \epsilon)$. Within this approximation, this expression is proportional to the current matrix in the Usadel equation, which can be seen when inserting it into the even equation. We want to include corrections to this result by including terms to the first order in the spin-orbit scattering strength. We assume that

$$\check{g}_{\text{av}}^p(\mathbf{R}, \epsilon) = -\tau v_F \check{g}_{\text{av}}^s(\mathbf{R}, \epsilon) \nabla_{\mathbf{R}} \check{g}_{\text{av}}^s(\mathbf{R}, \epsilon) + \delta \check{g}_{\text{av}}^p(\mathbf{R}, \epsilon), \quad (52)$$

and insert this back into the odd equation. We assume that $|\check{g}_{\text{av}}^{\text{p}}(\mathbf{R}, \epsilon)| \ll \check{g}_{\text{av}}^{\text{s}}(\mathbf{R}, \epsilon)$ and neglect terms of second order in $\check{g}_{\text{av}}^{\text{p}}(\mathbf{R}, \epsilon)$ as well as terms with one $\check{g}_{\text{av}}^{\text{p}}(\mathbf{R}, \epsilon)$ and one $\nabla_{\mathbf{R}}\check{g}_{\text{av}}^{\text{s}}(\mathbf{R}, \epsilon)$. We arrive at a correction

$$\begin{aligned} \delta\check{g}_{\text{av}}^{\text{p}}(\mathbf{R}, \epsilon) = & \left(\frac{\alpha p_{\text{F}}}{2} - \frac{\alpha v_{\text{F}} p_{\text{F}}^2 \tau^2}{3\tau_{\text{sk}}} \right) [\hat{\rho}_3 \hat{\sigma} \times \nabla_{\mathbf{R}} \check{g}_{\text{av}}^{\text{s}}(\mathbf{R}, \epsilon)] \\ & - \left(\frac{i\alpha v_{\text{F}} p_{\text{F}}^2 \tau}{3} + \frac{i\alpha p_{\text{F}} \tau}{2\tau_{\text{sk}}} \right) \{ \hat{\rho}_3 \hat{\sigma} \times \check{g}_{\text{av}}^{\text{s}}(\mathbf{R}, \epsilon) \nabla_{\mathbf{R}} \check{g}_{\text{av}}^{\text{s}}(\mathbf{R}, \epsilon) \}. \end{aligned} \quad (53)$$

Above, we have introduced

$$1/\tau = 2\pi n N_0 \langle |u(\mathbf{e}_{p_{\text{F}}} - \mathbf{e}_{q_{\text{F}}})|^2 \rangle_{p_{\text{F}}, q_{\text{F}}}, \quad (54)$$

$$1/\tau_{\text{sk}} = 2\pi^2 n N_0^2 \langle u(\mathbf{e}_{p_{\text{F}}} - \mathbf{e}_{q_{\text{F}}}) u(\mathbf{e}_{q_{\text{F}}} - \mathbf{e}_{q'_{\text{F}}}) u(\mathbf{e}_{q'_{\text{F}}} - \mathbf{e}_{p_{\text{F}}}) \rangle_{p_{\text{F}}, q_{\text{F}}, q'_{\text{F}}}. \quad (55)$$

Note that the requirement $\{\delta\check{g}_{\text{av}}^{\text{p}}(\mathbf{R}, \epsilon), \check{g}_{\text{av}}^{\text{s}}(\mathbf{R}, \epsilon)\} = 0$ ensures that the Green's function follows the normalization condition. The above expression for $\check{g}_{\text{av}}^{\text{p}}(\mathbf{R}, \epsilon)$ is inserted into the even equation to arrive at the Usadel equation.

The final step is to evaluate the even equation. The contribution from the odd equation enters the even equation through the term

$$\begin{aligned} \frac{i v_{\text{F}}}{3} \nabla_{\mathbf{R}} \cdot \check{g}_{\text{av}}^{\text{p}}(\mathbf{R}, \epsilon) = & - \frac{i v_{\text{F}}^2 \tau}{3} \nabla_{\mathbf{R}} \cdot [\check{g}_{\text{av}}^{\text{s}}(\mathbf{R}, \epsilon) \nabla_{\mathbf{R}} \check{g}_{\text{av}}^{\text{s}}(\mathbf{R}, \epsilon)] \\ & + \left(\frac{i\alpha v_{\text{F}} p_{\text{F}}}{6} - \frac{i\alpha v_{\text{F}}^2 p_{\text{F}}^2 \tau^2}{9\tau_{\text{sk}}} \right) \nabla_{\mathbf{R}} \cdot [\hat{\rho}_3 \hat{\sigma} \times \nabla_{\mathbf{R}} \check{g}_{\text{av}}^{\text{s}}(\mathbf{R}, \epsilon)] \\ & + \left(\frac{\alpha v_{\text{F}}^2 p_{\text{F}}^2 \tau}{9} + \frac{\alpha v_{\text{F}} p_{\text{F}} \tau}{6\tau_{\text{sk}}} \right) \nabla_{\mathbf{R}} \cdot \{ \hat{\rho}_3 \hat{\sigma} \times \check{g}_{\text{av}}^{\text{s}}(\mathbf{R}, \epsilon) \nabla_{\mathbf{R}} \check{g}_{\text{av}}^{\text{s}}(\mathbf{R}, \epsilon) \}. \end{aligned} \quad (56)$$

Because we have added extra $\mathcal{O}(\alpha^1)$ terms containing a gradient of the Green's function in the odd equation, we need to include terms up to order $\mathcal{O}\{\nabla_{\mathbf{R}} \check{g}_{\text{av}}^{\text{s}}(\mathbf{R}, \epsilon) \times \nabla_{\mathbf{R}} \check{g}_{\text{av}}^{\text{s}}(\mathbf{R}, \epsilon)\}$ in the gradients for the $\mathcal{O}(\alpha^0)$ and $\mathcal{O}(\alpha^1)$ terms in the even equation. This is the reason why we need to consider first order terms in the gradient approximation in the even equation [38]. Moreover, we assume that $l_{(\text{sk})} = \sqrt{D\tau_{(\text{sk})}} \gg p_{\text{F}}^{-1}$, which implies that $v_{\text{F}} p_{\text{F}} \gg \tau_{(\text{sk})}^{-1}$. This allows us to neglect terms that goes like $\alpha/\tau_{(\text{sk})}$. The contributions from the self-energy terms in the even equation in Eq. (38) are:

1) There is no contribution from $\check{\sigma}^{u^2}(\mathbf{R}, \mathbf{p}, \epsilon)$.

2) The contribution from $\check{\sigma}^{u u_{\text{so}}}(\mathbf{R}, \mathbf{p}, \epsilon)$ is

$$\begin{aligned} & \frac{i\alpha v_{\text{F}} p_{\text{F}}}{6} \nabla_{\mathbf{R}} \cdot [\hat{\rho}_3 \hat{\sigma} \times \nabla_{\mathbf{R}} \check{g}_{\text{av}}^{\text{s}}(\mathbf{R}, \epsilon)] + \frac{\alpha v_{\text{F}}^2 p_{\text{F}}^2 \tau}{18} [\hat{\rho}_3 \hat{\sigma} ; [\nabla_{\mathbf{R}} \check{g}_{\text{av}}^{\text{s}}(\mathbf{R}, \epsilon)] \times [\nabla_{\mathbf{R}} \check{g}_{\text{av}}^{\text{s}}(\mathbf{R}, \epsilon)]] \\ & + \frac{i\alpha v_{\text{F}} p_{\text{F}} \tau}{6} [\hat{\rho}_3 \hat{\sigma} ; \check{g}_{\text{av}}^{\text{s}}(\mathbf{R}, \epsilon) [\nabla_{\mathbf{R}} \check{g}_{\text{av}}^{\text{s}}(\mathbf{R}, \epsilon)] \times [\nabla_{\mathbf{R}} \check{g}_{\text{av}}^{\text{s}}(\mathbf{R}, \epsilon)]] \end{aligned} \quad (57)$$

3) The contribution from $\check{\sigma}^{u_{\text{so}}^2}(\mathbf{R}, \mathbf{p}, \epsilon)$ is

$$\frac{i\alpha^2 p_{\text{F}}^4}{9\tau} [\hat{\rho}_3 \hat{\sigma} \cdot \check{g}_{\text{av}}^{\text{s}}(\mathbf{R}, \epsilon) \hat{\rho}_3 \hat{\sigma} \cdot \check{g}_{\text{av}}^{\text{s}}(\mathbf{R}, \epsilon)]. \quad (58)$$

4) There is no contribution from $\check{\sigma}^{u^3}(\mathbf{R}, \mathbf{p}, \epsilon)$.

5) The contribution from $\check{\sigma}^{u^2 u_{\text{so}}}(\mathbf{R}, \mathbf{p}, \epsilon)$ is

$$\begin{aligned} & \frac{\alpha v_{\text{F}} p_{\text{F}} \tau}{12\tau_{\text{sk}}} \nabla_{\mathbf{R}} \cdot \{ \hat{\rho}_3 \hat{\sigma} \times \check{g}_{\text{av}}^{\text{s}}(\mathbf{R}, \epsilon) \nabla_{\mathbf{R}} \check{g}_{\text{av}}^{\text{s}}(\mathbf{R}, \epsilon) \} + \frac{\alpha v_{\text{F}} p_{\text{F}} \tau}{8\tau_{\text{sk}}} [\hat{\rho}_3 \hat{\sigma} ; [\nabla_{\mathbf{R}} \check{g}_{\text{av}}^{\text{s}}(\mathbf{R}, \epsilon)] \times [\nabla_{\mathbf{R}} \check{g}_{\text{av}}^{\text{s}}(\mathbf{R}, \epsilon)]] \\ & - \frac{i\alpha v_{\text{F}}^2 p_{\text{F}}^2 \tau^2}{18\tau_{\text{sk}}} [\hat{\rho}_3 \hat{\sigma} ; \check{g}_{\text{av}}^{\text{s}}(\mathbf{R}, \epsilon) [\nabla_{\mathbf{R}} \check{g}_{\text{av}}^{\text{s}}(\mathbf{R}, \epsilon)] \times [\nabla_{\mathbf{R}} \check{g}_{\text{av}}^{\text{s}}(\mathbf{R}, \epsilon)]]. \end{aligned} \quad (59)$$

6) The contribution from $\check{\sigma}^{u_{\text{sf}}^2}(\mathbf{R}, \mathbf{p}, \epsilon)$ is

$$\frac{iS(S+1)}{18\tau_{\text{m}}} [\hat{\sigma} \cdot \check{g}_{\text{av}}^{\text{s}}(\mathbf{R}, \epsilon) \hat{\sigma} \cdot \check{g}_{\text{av}}^{\text{s}}(\mathbf{R}, \epsilon)], \quad (60)$$

where we defined

$$1/\tau_{\text{m}} = 2\pi n_{\text{m}} N_0 \langle |u_{\text{m}}(\mathbf{e}_{p_{\text{F}}} - \mathbf{e}_{q_{\text{F}}})|^2 \rangle_{p_{\text{F}}, q_{\text{F}}}. \quad (61)$$

Adding up all terms, we arrive at the Usadel equation in the main text. In this equation, we have additionally included inelastic scattering in the relaxation time approximation which can be thought of as a constant tunneling coupling to an infinite normal-metal reservoir.

As an important test to our solution, we show that the Usadel equation can be written in a commutator form. We evaluate the divergence of the matrix current, and find that

$$\begin{aligned} \nabla_{\mathbf{R}} \cdot \tilde{\mathbf{J}}(\mathbf{R}, \epsilon) &= \tilde{\mathcal{J}}(\mathbf{R}, \epsilon) + \frac{1}{2} [D \nabla_{\mathbf{R}}^2 \tilde{g}_{\text{av}}^s(\mathbf{R}, \epsilon) \\ &+ (\nabla_{\mathbf{R}} \cdot \tilde{\mathbf{J}}^{(1)}(\mathbf{R}, \epsilon)) \tilde{g}_{\text{av}}^s(\mathbf{R}, \epsilon) + \frac{D\theta}{2} [\nabla_{\mathbf{R}} \tilde{g}_{\text{av}}^s(\mathbf{R}, \epsilon)] \cdot [\hat{\rho}_3 \hat{\sigma} \times \nabla_{\mathbf{R}} \tilde{g}_{\text{av}}^s(\mathbf{R}, \epsilon)], \tilde{g}_{\text{av}}^s(\mathbf{R}, \epsilon)]. \end{aligned} \quad (62)$$

By inserting this expression into the Usadel equation, we realize that it ensures that the Usadel equation can be written as a commutator with $\tilde{g}_{\text{av}}^s(\mathbf{R}, \epsilon)$.

In the Usadel equation in the main text, we have for simplicity only defined the quantities that are important for our main results. For completeness, we here give the remaining expressions. The torque is given by

$$\tilde{\mathcal{J}}(\mathbf{R}, \epsilon) = -\frac{D\theta}{4} [\hat{\rho}_3 \hat{\sigma} ; \tilde{g}_{\text{av}}^s(\mathbf{R}, \epsilon) (\nabla_{\mathbf{R}} \tilde{g}_{\text{av}}^s(\mathbf{R}, \epsilon) \times (\nabla_{\mathbf{R}} \tilde{g}_{\text{av}}^s(\mathbf{R}, \epsilon))] - \frac{iD\kappa}{4} [\hat{\rho}_3 \hat{\sigma} ; (\nabla_{\mathbf{R}} \tilde{g}_{\text{av}}^s(\mathbf{R}, \epsilon) \times (\nabla_{\mathbf{R}} \tilde{g}_{\text{av}}^s(\mathbf{R}, \epsilon))]. \quad (63)$$

By evaluating its Keldysh component, we see that it only contributes to transport when the retarded Green's function is spatially dependent. The spin-Hall and spin-swap angles in the normal-state are given by

$$\theta = -\frac{2\alpha p_F^2 \tau}{3\tau_{\text{sk}}} + \frac{2\alpha p_F}{v_F \tau}, \quad \kappa = -\frac{2\alpha p_F^2}{3} - \frac{3\alpha p_F}{2v_F \tau_{\text{sk}}}. \quad (64)$$

Furthermore, the scattering times associated with spin-flip and spin-orbit scattering are given by

$$1/\tau_{\text{sf}} = 8\pi n_{\text{m}} N_0 \langle |u_{\text{m}}(\mathbf{e}_{p_F} - \mathbf{e}_{q_F})|^2 \rangle_{p_F, q_F} S(S+1)/3, \quad (65)$$

$$1/\tau_{\text{so}} = 8\alpha^2 p_F^4 / (9\tau). \quad (66)$$

II. The kinetic equations

In order to calculate the currents and the non-equilibrium charge and spin accumulations, we must solve the kinetic equations. These are obtained by evaluating the Keldysh part of the Usadel equation derived in the previous section. We first assume that the retarded Green's function is equal to its equilibrium value

$$\hat{g}_{\text{av}}^{\text{R}}(\epsilon) = \begin{pmatrix} g_+(\epsilon) & 0 & 0 & f_s(\epsilon) + f_t(\epsilon) \\ 0 & g_-(\epsilon) & -f_s(\epsilon) + f_t(\epsilon) & 0 \\ 0 & f_s(\epsilon) - f_t(\epsilon) & -g_-(\epsilon) & 0 \\ -f_s(\epsilon) - f_t(\epsilon) & 0 & 0 & -g_+(\epsilon) \end{pmatrix}, \quad (67)$$

where

$$g_{\pm}(\epsilon) = (\epsilon + i\delta \pm m)I^{\pm}(\epsilon), \quad f_s(\epsilon) = \frac{\Delta}{2} [I^+(\epsilon) + I^-(\epsilon)], \quad f_t(\epsilon) = \frac{\Delta}{2} [I^+(\epsilon) - I^-(\epsilon)] \quad (68)$$

are the spin-split ordinary retarded Green's functions, and the spin-singlet and spin-triplet parts of the anomalous retarded Green's function, respectively. Above, m is the magnitude of the spin-splitting field $\mathbf{m} = m\mathbf{z}$, δ is small and related to the strength of the inelastic scattering, and

$$I^{\pm}(\epsilon) = \frac{\text{sgn}(\epsilon \pm m)}{\sqrt{(\epsilon + i\delta \pm m)^2 - |\Delta|^2}} \Theta((\epsilon \pm m)^2 - |\Delta|^2) - \frac{i}{\sqrt{|\Delta|^2 - (\epsilon + i\delta \pm m)^2}} \Theta(|\Delta|^2 - (\epsilon \pm m)^2). \quad (69)$$

Assuming an equilibrium Green's function makes it possible to obtain analytic expressions. This assumption is justifiable as long as there is no conversion between quasi-particle currents and supercurrents. Local suppression of the anomalous Green's function close to the interface can be neglected as it will not cause qualitative changes in the quasi-particle currents.

The aim of solving the kinetic equations is to determine the non-equilibrium properties of the Green's function. We relate the advanced and Keldysh Green's functions to the retarded one by

$$\hat{g}_{\text{av}}^{\text{A}}(\epsilon) = -[\hat{\rho}_3 \hat{g}_{\text{av}}^{\text{R}}(\epsilon) \hat{\rho}_3]^{\dagger}, \quad \hat{g}_{\text{av}}^{\text{K}}(\epsilon) = \hat{g}_{\text{av}}^{\text{R}}(\epsilon) \hat{h}(\mathbf{R}, \epsilon) - \hat{h}(\mathbf{R}, \epsilon) \hat{g}_{\text{av}}^{\text{A}}(\epsilon), \quad (70)$$

where the distribution function matrix

$$\hat{h}(\mathbf{R}, \epsilon) = \hat{\rho}_0 h_L(\mathbf{R}, \epsilon) + \hat{\rho}_3 h_T(\mathbf{R}, \epsilon) + \sum_i \hat{\sigma}_i h_{LSi}(\mathbf{R}, \epsilon) + \sum_i \hat{\rho}_3 \hat{\sigma}_i h_{TSi}(\mathbf{R}, \epsilon) \quad (71)$$

describes the non-equilibrium energy distribution $h_L(\mathbf{R}, \epsilon)$, charge distribution $h_T(\mathbf{R}, \epsilon)$, spin-energy distribution $h_{LSi}(\mathbf{R}, \epsilon)$, and spin distribution $h_{TSi}(\mathbf{R}, \epsilon)$. These can be found by performing appropriate traces over the distribution function matrix $\hat{h}(\mathbf{R}, \epsilon)$. Performing the corresponding traces on the Keldysh part of the matrix current $\hat{\mathbf{J}}(\mathbf{R}, \epsilon)$, we obtain the energy resolved energy current $\mathbf{j}_L(\mathbf{R}, \epsilon)$, charge current $\mathbf{j}_T(\mathbf{R}, \epsilon)$, spin-energy current $\mathbf{j}_{LSi}(\mathbf{R}, \epsilon)$, and spin current $\mathbf{j}_{TSi}(\mathbf{R}, \epsilon)$. We separate these currents into a zeroth order and a first order contribution in the spin-orbit parameter α . The zeroth order currents are related to the distribution functions by

$$\mathbf{j}_L^{(0)}(\mathbf{R}, \epsilon) = -2 [D_L(\epsilon) \nabla_{\mathbf{R}} h_L(\mathbf{R}, \epsilon) + D_{TSz}(\epsilon) \nabla_{\mathbf{R}} h_{TSz}(\mathbf{R}, \epsilon)], \quad (72)$$

$$\mathbf{j}_{TSx}^{(0)}(\mathbf{R}, \epsilon) = -2 [D_{TSx}(\epsilon) \nabla_{\mathbf{R}} h_{TSx}(\mathbf{R}, \epsilon) + D_{TSy}(\epsilon) \nabla_{\mathbf{R}} h_{TSy}(\mathbf{R}, \epsilon)], \quad (73)$$

$$\mathbf{j}_{TSy}^{(0)}(\mathbf{R}, \epsilon) = -2 [D_{TSx}(\epsilon) \nabla_{\mathbf{R}} h_{TSy}(\mathbf{R}, \epsilon) - D_{TSy}(\epsilon) \nabla_{\mathbf{R}} h_{TSx}(\mathbf{R}, \epsilon)], \quad (74)$$

$$\mathbf{j}_{TSz}^{(0)}(\mathbf{R}, \epsilon) = -2 [D_L(\epsilon) \nabla_{\mathbf{R}} h_{TSz}(\mathbf{R}, \epsilon) + D_{TSz}(\epsilon) \nabla_{\mathbf{R}} h_L(\mathbf{R}, \epsilon)]. \quad (75)$$

The first order currents are transversal to the zeroth order currents. The relevant first order currents are expressed in terms of the zeroth order currents in the main text. The coefficients are given by

$$D_L(\epsilon) = \frac{D}{2} \left\{ 1 + \frac{1}{2} [|g_+(\epsilon)|^2 + |g_-(\epsilon)|^2 - 2|f_s(\epsilon)|^2 - 2|f_t(\epsilon)|^2] \right\} \quad (76)$$

$$D_{TSx}(\epsilon) = \frac{D}{2} \{ 1 + \text{Re}\{g_+(\epsilon)[g_-(\epsilon)]^*\} - |f_s(\epsilon)|^2 + |f_t(\epsilon)|^2 \} \quad (77)$$

$$D_{TSy}(\epsilon) = \frac{D}{2} (\Im\{g_+(\epsilon)[g_-(\epsilon)]^*\} + \Im\{f_s(\epsilon)[f_t(\epsilon)]^*\}), \quad (78)$$

$$D_{TSz}(\epsilon) = \frac{D}{4} [|g_+(\epsilon)|^2 - |g_-(\epsilon)|^2 - 4\text{Re}\{f_s(\epsilon)[f_t(\epsilon)]^*\}]. \quad (79)$$

We also define

$$N_{\pm}(\epsilon) = \{\text{Re}[g_+(\epsilon)] \pm \text{Re}[g_-(\epsilon)]\}/2, \quad (80)$$

$$N_{\pm}^I(\epsilon) = \{\Im[g_+(\epsilon)] - \Im[g_-(\epsilon)]\}/2 \quad (81)$$

in order to express the first order currents in the main text. Above, $N_0 N_+(\epsilon)$ is the density-of-states.

We have now obtained analytic expressions for the first order currents in terms of the zeroth order ones. To evaluate the zeroth order currents, we must solve the kinetic equations for the injected energy and spin currents numerically. The kinetic equations are given by

$$\nabla_{\mathbf{R}} \cdot \mathbf{j}_L^{(0)}(\mathbf{R}, \epsilon) = -4\delta \left\{ N_+(\epsilon) \left[h_L(\mathbf{R}, \epsilon) - \tanh\left(\frac{\epsilon}{2T}\right) \right] + N_-(\epsilon) h_{TSz}(\mathbf{R}, \epsilon) \right\}, \quad (82)$$

$$\nabla_{\mathbf{R}} \cdot \mathbf{j}_{TSz}^{(0)}(\mathbf{R}, \epsilon) = -2 \left[\frac{\alpha_{so}(\epsilon)}{\tau_{so}} + \frac{\alpha_{sf}(\epsilon)}{\tau_{sf}} \right] h_{TSz}(\mathbf{R}, \epsilon) - 4\delta \left\{ N_+(\epsilon) h_{TSz}(\mathbf{R}, \epsilon) + N_-(\epsilon) \left[h_L(\mathbf{R}, \epsilon) - \tanh\left(\frac{\epsilon}{2T}\right) \right] \right\}, \quad (83)$$

$$\begin{aligned} \nabla_{\mathbf{R}} \cdot \mathbf{j}_{TSx}^{(0)}(\mathbf{R}, \epsilon) = & 4m[N_-^I(\epsilon) h_{TSx}(\mathbf{R}, \epsilon) - N_+(\epsilon) h_{TSy}(\mathbf{R}, \epsilon)] \\ & - 2 \left[\frac{\alpha_{so}^x(\epsilon)}{\tau_{so}} + \frac{\alpha_{sf}^x(\epsilon)}{\tau_{sf}} \right] h_{TSx}(\mathbf{R}, \epsilon) - 2 \left[\frac{\alpha_{so}^y(\epsilon)}{\tau_{so}} + \frac{\alpha_{sf}^y(\epsilon)}{\tau_{sf}} \right] h_{TSy}(\mathbf{R}, \epsilon) \\ & - 4\delta [N_+(\epsilon) h_{TSx}(\mathbf{R}, \epsilon) + N_-^I(\epsilon) h_{TSy}(\mathbf{R}, \epsilon)], \end{aligned} \quad (84)$$

$$\begin{aligned} \nabla_{\mathbf{R}} \cdot \mathbf{j}_{TSy}^{(0)}(\mathbf{R}, \epsilon) = & 4m[N_-^I(\epsilon) h_{TSy}(\mathbf{R}, \epsilon) + N_+(\epsilon) h_{TSx}(\mathbf{R}, \epsilon)] \\ & - 2 \left[\frac{\alpha_{so}^x(\epsilon)}{\tau_{so}} + \frac{\alpha_{sf}^x(\epsilon)}{\tau_{sf}} \right] h_{TSy}(\mathbf{R}, \epsilon) + 2 \left[\frac{\alpha_{so}^y(\epsilon)}{\tau_{so}} + \frac{\alpha_{sf}^y(\epsilon)}{\tau_{sf}} \right] h_{TSx}(\mathbf{R}, \epsilon) \\ & - 4\delta [N_+(\epsilon) h_{TSy}(\mathbf{R}, \epsilon) - N_-^I(\epsilon) h_{TSx}(\mathbf{R}, \epsilon)], \end{aligned} \quad (85)$$

where

$$\alpha_{\text{so}}(\epsilon) = \text{Re}[g_{\uparrow}(\epsilon)]\text{Re}[g_{\downarrow}(\epsilon)] - \{\text{Re}[f_s(\epsilon)]\}^2 + \{\text{Re}[f_t(\epsilon)]\}^2 \quad (86)$$

$$\alpha_{\text{sf}}(\epsilon) = \text{Re}[g_{\uparrow}(\epsilon)]\text{Re}[g_{\downarrow}(\epsilon)] + \{\text{Re}[f_s(\epsilon)]\}^2 - \{\text{Re}[f_t(\epsilon)]\}^2, \quad (87)$$

$$\alpha_{\text{so}}^x(\epsilon) = [N_+(\epsilon)]^2 - \{\text{Re}[f_s(\epsilon)]\}^2, \quad (88)$$

$$\alpha_{\text{so}}^y(\epsilon) = \{\text{Re}[g_+(\epsilon)]\Im[g_+(\epsilon)] - \text{Re}[g_-(\epsilon)]\Im[g_-(\epsilon)] - \Im[g_+(\epsilon)g_-^*(\epsilon)] - 4\text{Re}[f_s(\epsilon)]\Im[f_t(\epsilon)]\} / 4, \quad (89)$$

$$\alpha_{\text{sf}}^x(\epsilon) = (\{\text{Re}[g_+(\epsilon)] + \text{Re}[g_-(\epsilon)]\}^2 + 4\{\text{Re}[f_s(\epsilon)]\}^2) / 4, \quad (90)$$

$$\alpha_{\text{sf}}^y(\epsilon) = (\{\Im[g_+(\epsilon) + g_-^*(\epsilon)]\}^2 / 4 + \Im[f_s(\epsilon)f_t(\epsilon)] - \Im[f_s(\epsilon)f_t^*(\epsilon)]) / 2. \quad (91)$$

We want to consider the dependence on temperature and spin-splitting. To do so, we assume that the superconducting pairing is equal to its value in a uniform spin-split superconductor. The gap equation for such a bulk superconductor is given by

$$\Delta = \frac{N_0 U}{2} \int d\epsilon \text{Re}[f_s(\epsilon)] \tanh\left(\frac{\epsilon}{2T}\right). \quad (92)$$

We solve this equation self-consistently with the Debye cutoff $\omega_D = \Delta_0 \cosh(1/N_0 U)$. In all figures, we use $\omega_D \approx 74\Delta_0$.

To solve the kinetic equations, we must define boundary conditions. We use the Kupriyanov-Lukichev boundary condition

$$\mathbf{n}_{1 \rightarrow 2} \cdot 2L_j \zeta_j [\hat{g}_{\text{av}}^s(\mathbf{R}, \epsilon)]_j \nabla_{\mathbf{R}} [\hat{g}_{\text{av}}^s(\mathbf{R}, \epsilon)]_j = [[\hat{g}_{\text{av}}^s(\mathbf{R}, \epsilon)]_1, [\hat{g}_{\text{av}}^s(\mathbf{R}, \epsilon)]_2], \quad (93)$$

where $\mathbf{n}_{1 \rightarrow 2}$ is the normal unit vector from material 1 to material 2, L_j is the length of material $j \in \{1, 2\}$ in the direction of the interface normal, and $\zeta_j = R_B/R_j$ is the ratio between the barrier resistance and the resistance of material j . In Fig. 3 in the main text, we have used $\zeta_{\text{SC}} = 4$. First consider a normal-metal/spin-split superconductor (NM/ssSC) interface at $x_i = 0$ where a z polarized spin-voltage $V_{\uparrow} = -V_{\downarrow} = V/2$ is applied to the NM. This corresponds to the boundary conditions

$$j_{\text{L}}^{i(0)}(0^+, \epsilon) = -\frac{D}{L_{\text{SC}}\zeta_{\text{SC}}} \{N_+(\epsilon)[h_{\text{L}}(0^+, \epsilon) - h_{\text{L}}(0^-, \epsilon)] + N_-(\epsilon)[h_{\text{TS}z}(0^+, \epsilon) - h_{\text{TS}z}(0^-, \epsilon)]\}, \quad (94)$$

$$j_{\text{TS}z}^{i(0)}(0^+, \epsilon) = -\frac{D}{L_{\text{SC}}\zeta_{\text{SC}}} \{N_+(\epsilon)[h_{\text{TS}z}(0^+, \epsilon) - h_{\text{TS}z}(0^-, \epsilon)] + N_-(\epsilon)[h_{\text{L}}(0^+, \epsilon) - h_{\text{L}}(0^-, \epsilon)]\}, \quad (95)$$

with

$$h_{\text{L}}(0^-, \epsilon) = \frac{1}{2} \left[\tanh\left(\frac{\epsilon + eV/2}{2T}\right) + \tanh\left(\frac{\epsilon - eV/2}{2T}\right) \right], \quad (96)$$

$$h_{\text{TS}z}(0^-, \epsilon) = \frac{1}{2} \left[\tanh\left(\frac{\epsilon + eV/2}{2T}\right) - \tanh\left(\frac{\epsilon - eV/2}{2T}\right) \right]. \quad (97)$$

If we instead consider an x polarized spin-voltage, the boundary condition at $x_i = 0$ is

$$j_{\text{L}}^{i(0)}(0^+, \epsilon) = -\frac{D}{L_{\text{SC}}\zeta_{\text{SC}}} \{N_+(\epsilon)[h_{\text{L}}(0^+, \epsilon) - h_{\text{L}}(0^-, \epsilon)] + N_-(\epsilon)h_{\text{TS}z}(0^+, \epsilon)\}, \quad (98)$$

$$j_{\text{TS}x}^{i(0)}(0^+, \epsilon) = -\frac{D}{L_{\text{SC}}\zeta_{\text{SC}}} \{N_+(\epsilon)[h_{\text{TS}x}(0^+, \epsilon) - h_{\text{TS}x}(0^-, \epsilon)] + N_-^{\text{I}}(\epsilon)h_{\text{TS}y}(0^+, \epsilon)\}, \quad (99)$$

$$j_{\text{TS}y}^{i(0)}(0^+, \epsilon) = -\frac{D}{L_{\text{SC}}\zeta_{\text{SC}}} \{N_+(\epsilon)h_{\text{TS}y}(0^+, \epsilon) - N_-^{\text{I}}(\epsilon)[h_{\text{TS}x}(0^+, \epsilon) - h_{\text{TS}x}(0^-, \epsilon)]\}, \quad (100)$$

$$j_{\text{TS}z}^{i(0)}(0^+, \epsilon) = -\frac{D}{L_{\text{SC}}\zeta_{\text{SC}}} \{N_+(\epsilon)h_{\text{TS}z}(0^+, \epsilon) + N_-(\epsilon)[h_{\text{L}}(0^+, \epsilon) - h_{\text{L}}(0^-, \epsilon)]\}, \quad (101)$$

with $h_{\text{L}}(0^-, \epsilon)$ following Eq. (96), and $h_{\text{TS}x}(0^-, \epsilon)$ being equal to $h_{\text{TS}z}(0^-, \epsilon)$ for the z polarized case (Eq. (97)). For the right interface at $x_i = L_{\text{SC}}$, we consider a ssSC/vacuum interface where all currents are zero.

The relevant length scales should obey $l \ll l_{\text{so}}, l_{\text{sf}} \ll l_{\text{isc}} < L_{\text{SC}}$. We have defined the scattering length for scattering on non-magnetic impurities as $l = \sqrt{D\tau}$ and the normal-state scattering length for spin-orbit (spin-flip) scattering as $l_{\text{so(sf)}} = \sqrt{D\tau_{\text{so(sf)}}}$. The normal-state inelastic scattering length is given by $l_{\text{isc}} = \sqrt{D/2\delta N_0}$. Additionally, a precession length can be defined as $l_{\text{prec}} = \sqrt{D/2mN_0}$ which is determined by the strength of the spin-splitting field. In Fig. 3 in the main text, we use $l_{\text{so}} = l_{\text{sf}} = 20l$, $l_{\text{isc}} = 250l$, and $L_{\text{SC}} = 2l_{\text{isc}}$. We consider an inelastic scattering parameter $\delta = 10^{-3}\Delta_0$, and use that $l_{\text{prec}} = \sqrt{\delta/m} l_{\text{isc}}$.

III. The non-equilibrium charge and spin accumulations

After solving the kinetic equations with a self-consistently determined gap Δ with the Kupriyanov-Lukichev boundary conditions described in the previous section, we can calculate the non-equilibrium charge and spin accumulations. In a spin-split superconductor, the charge accumulation $\mu(x_j)$, and the i polarized spin accumulations $\mu_i^s(x_j)$ are given by

$$\frac{\mu(x_j)}{e} = -\frac{1}{2} \int d\epsilon \{N_+(\epsilon)h_T(x_j, \epsilon) + N_-(\epsilon)h_{LSz}(x_j, \epsilon)\}, \quad (102)$$

$$\frac{\mu_x^s(x_j)}{1/2} = -\frac{1}{2} \int d\epsilon \{N_+(\epsilon)h_{TSx}(x_j, \epsilon) + N_-^I(\epsilon)h_{TSy}(x_j, \epsilon)\}, \quad (103)$$

$$\frac{\mu_y^s(x_j)}{1/2} = -\frac{1}{2} \int d\epsilon \{N_+(\epsilon)h_{TSy}(x_j, \epsilon) - N_-^I(\epsilon)h_{TSx}(x_j, \epsilon)\}, \quad (104)$$

$$\frac{\mu_z^s(x_j)}{1/2} = -\frac{1}{2} \int d\epsilon \left\{ N_+(\epsilon)h_{TSz}(x_j, \epsilon) + N_-(\epsilon) \left[h_L(x_j, \epsilon) - \tanh\left(\frac{\epsilon}{2T}\right) \right] \right\}, \quad (105)$$

for $i = x, y, z$. We want to find the resulting charge and spin accumulation across the superconductor due to the transversal currents. If we measure the voltage or spin-voltage, the current going through the measuring circuit is negligible. We therefore require that there is no net transversal current at the edges of the sample. A current is induced between the edges of the sample to compensate for the first order transversal current. Our boundary condition is a complete cancellation of these currents at the edges. We assume that the width W of the superconductor is short enough that there is no conversion between quasi-particle and supercurrent, and that there is no significant scattering apart from the ordinary scattering on non-magnetic impurities. We also assume that the coupling between the x and y polarized spin currents is weak so that the precession around the spin-splitting field is slow compared to the time it takes for the spin current to cross the width of the sample. The relative charge accumulation $\Delta\mu(x_i) = \mu(x_i, W/2) - \mu(x_i, -W/2)$ across the spin-split superconductor is given by

$$\Delta\mu(x_i) = -\frac{W}{2} \int d\epsilon \left\{ \frac{N_+(\epsilon)D_T(\epsilon) - N_-(\epsilon)D_{LSz}(\epsilon)}{[D_T(\epsilon)]^2 - [D_{LSz}(\epsilon)]^2} j_T^{j(1)}(x_i, \epsilon) - \frac{N_+(\epsilon)D_{LSz}(\epsilon) - N_-(\epsilon)D_T(\epsilon)}{[D_T(\epsilon)]^2 - [D_{LSz}(\epsilon)]^2} j_{LSz}^{j(1)}(x_i, \epsilon) \right\}, \quad (106)$$

where x_i is the distance from the normal-metal contact, and

$$D_T(\epsilon) = \frac{D}{2} \left\{ 1 + \frac{1}{2} [|g_+(\epsilon)|^2 + |g_-(\epsilon)|^2 + 2|f_s(\epsilon)|^2 + 2|f_t(\epsilon)|^2] \right\}, \quad (107)$$

$$D_{LSz}(\epsilon) = \frac{D}{4} [|g_+(\epsilon)|^2 - |g_-(\epsilon)|^2 + 4\text{Re}\{f_s(\epsilon)[f_t(\epsilon)]^*\}]. \quad (108)$$

The relative non-equilibrium spin accumulations $\Delta\mu_S^j(x_i) = \mu_S^j(x_i, W/2) - \mu_S^j(x_i, -W/2)$ across the spin-split superconductor are given by

$$\Delta\mu_S^x(x_i) = -\frac{W}{2} \int d\epsilon \left\{ \frac{N_+(\epsilon)D_{TSx}(\epsilon) + N_-^I(\epsilon)D_{TSy}(\epsilon)}{[D_{TSx}(\epsilon)]^2 + [D_{TSy}(\epsilon)]^2} j_{TSx}^{j(1)}(x_i, \epsilon) - \frac{N_+(\epsilon)D_{TSy}(\epsilon) - N_-^I(\epsilon)D_{TSx}(\epsilon)}{[D_{TSx}(\epsilon)]^2 + [D_{TSy}(\epsilon)]^2} j_{TSy}^{j(1)}(x_i, \epsilon) \right\}, \quad (109)$$

$$\Delta\mu_S^y(x_i) = -\frac{W}{2} \int d\epsilon \left\{ \frac{N_+(\epsilon)D_{TSx}(\epsilon) + N_-^I(\epsilon)D_{TSy}(\epsilon)}{[D_{TSx}(\epsilon)]^2 + [D_{TSy}(\epsilon)]^2} j_{TSy}^{j(1)}(x_i, \epsilon) + \frac{N_+(\epsilon)D_{TSy}(\epsilon) - N_-^I(\epsilon)D_{TSx}(\epsilon)}{[D_{TSx}(\epsilon)]^2 + [D_{TSy}(\epsilon)]^2} j_{TSx}^{j(1)}(x_i, \epsilon) \right\}, \quad (110)$$

$$\Delta\mu_S^z(x_i) = -\frac{W}{2} \int d\epsilon \left\{ \frac{N_+(\epsilon)D_L(\epsilon) - N_-(\epsilon)D_{TSz}(\epsilon)}{[D_L(\epsilon)]^2 - [D_{TSz}(\epsilon)]^2} j_L^{j(1)}(x_i, \epsilon) - \frac{N_+(\epsilon)D_{TSz}(\epsilon) - N_-(\epsilon)D_L(\epsilon)}{[D_L(\epsilon)]^2 - [D_{TSz}(\epsilon)]^2} j_{TSz}^{j(1)}(x_i, \epsilon) \right\}. \quad (111)$$

We have absorbed a normalization factor e into the relative charge accumulation, and a factor $1/2$ into the relative spin accumulations for simplicity of notation.